THE UNIVERSITY OF ALABAMA® | University Libraries

Inner Ring Structures in Galaxies as Distance Indicators. I - Dimensionless Systematics of Inner Rings

R. Buta – University of Texas at Austin

G. de Vaucouleurs – University of Texas at Austin

Deposited 08/01/2019

Citation of published version:

Buta, R., de Vaucouleurs, G., (1980): Inner Ring Structures in Galaxies as Distance Indicators. I - Dimensionless Systematics of Inner Rings. *The Astrophysical Journal Supplement Series,* vol. 44. DOI: https://doi.org/10.1086/190700

© 1980. The American Astronomical Society. All rights reserved.

1980ApJS...44..451D

THE ASTROPHYSICAL JOURNAL SUPPLEMENT SERIES, 44: 451–479, 1980 December
© 1980. The American Astronomical Society. All rights reserved. Printed in U.S.A.

INNER RING STRUCTURES IN GALAXIES AS DISTANCE INDICATORS. I. DIMENSIONLESS SYSTEMATICS OF INNER RINGS

G. DE VAUCOULEURS AND R. BUTA
Department of Astronomy and McDonald Observatory, The University of Texas
Received 1980 March 3; accepted 1980 May 19

ABSTRACT

Inner ring structures are observed in about one quarter of all lenticular or spiral galaxies. Statistics of the relative frequencies of the pure ring (r) and broken ring (rs) *varieties* in the *Second Reference Catalogue* (RC2) among the different *families* (A, AB, B) of lenticular (L) and spiral (S) galaxies at different *stages* (T) along the revised Hubble sequence are presented; selection effects dependent on classification weight, apparent diameter and axis ratio are discussed. Comparisons of ring diameters D_r listed in the (First) *Reference Catalogue* (RC1) with independent measurements of 43 barred systems by Kormendy show good systematic agreement with a standard deviation $\sigma_{12}(D_r)=0.10$ and individual relative mean errors $\sigma(D_r)/\langle D_r\rangle\approx 5\%$. Axis ratios are also in good agreement with $\sigma_{12}(b/a)=0.06$. Comparisons of axis ratios of rings and parent galaxies show systematic trends dependent on stage T; in general rings have a greater ellipticity than the galaxy, particularly in early type galaxies, which suggests that rings are flatter than the galaxy, particularly its spheroidal component, and, at least in barred systems, are intrinsically elongated.

Statistics of the dimensionless parameters $X=\log D_0/D_r$, and $Y=\log A_e/D_r$, measuring the ratios of the galaxy diameters D_0 (isophotal) and A_e (metric) to the ring diameter D_r, are analyzed as functions of family (F), stage (T), variety (r versus rs), and luminosity class (L_c). No significant dependence on the latter two variables is indicated, but highly significant dependence on F and T is present:

$$X=\log D_0/D_r\approx 0.53-0.13F+0.04T,$$

$$Y=\log A_e/D_r\approx 0.01-0.13F+0.06T,$$

where $-1\leq F\leq +1$ for SA, SAB, SB, and $-2\leq T\leq +8$ from intermediate L to late S. Rings are relatively small in ordinary spirals (SA) and large in barred spirals (SB), and smaller in late types (S) than in early types (L). X and Y are shown to be a quantitative measure of bar strength underlying the classification concept of "family". An application to our Galaxy for which $D_0=23$ kpc, $A_e=10$ kpc, and $D_r=6$ kpc confirms its classification as SA$\underline{\text{B}}$ ($\underline{r}$s) previously derived from photometry.

The linear diameter of rings in spirals implied by this analysis is a function of F, T, and L_c, which will be calibrated in Paper II for use as a quaternary distance indicator.

Subject heading : galaxies: structure

I. INTRODUCTION

Spiral (S) and lenticular (S0≡L) galaxies often show well-defined inner ring structures which were first discussed by Randers (1940) and are recognized in the revised Hubble classification system by the differentiation of the (r) *variety* (de Vaucouleurs 1956*b*, 1959*c*; Sandage 1961, 1975). In lenticular galaxies the (r) structure is normally smooth and is located inside or more often at the outer edge of the lens (Kormendy 1979); examples are listed in Table 1 and illustrated in Figures 1–3 (Plates 13–15); in extreme cases, e.g., in NGC 7702, the aspect is reminiscent of Saturn's rings. In spiral galaxies the ring structure is usually made up of a large number of tightly coiled spiral arcs; in general the main spiral arms emerge tangentially at the periphery of the ring which envelops the bar in barred spirals; examples are given in Table 1 and illustrated in Figures 1–3.

In many galaxies the ring structure is broken up, incomplete, or weak and this fact is recognized by the notation (rs) for pseudorings in the revised classification system to designate the transition between the (r) and (s) *varieties* which occur in both the ordinary (SA) and barred (SB) spiral *families* as well as in the transition (SAB) type. In the latter-type, the inner, incom-

© American Astronomical Society • Provided by the NASA Astrophysics Data System

1980ApJS...44..451D

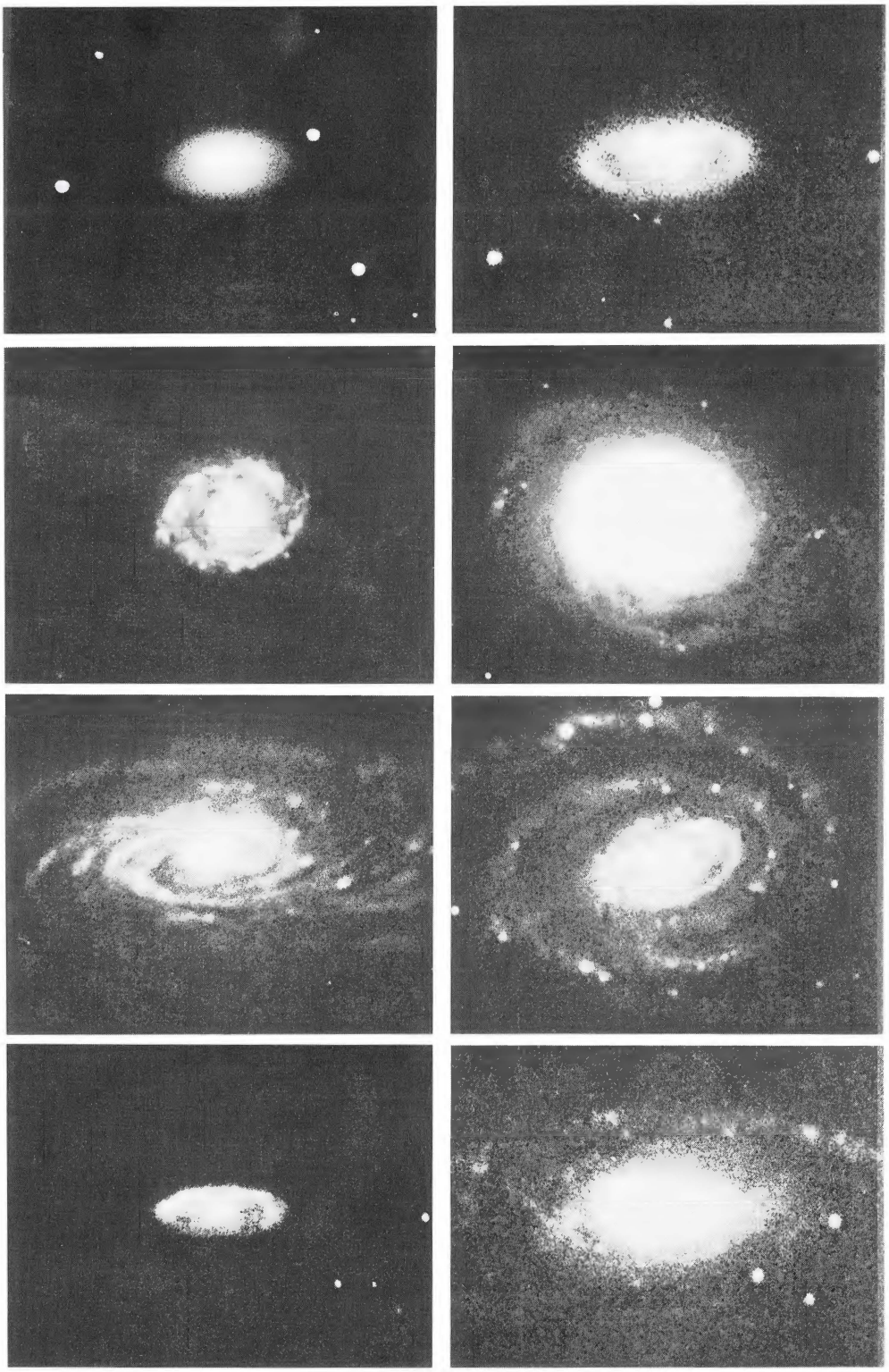

FIG. 1.—Examples of ordinary spiral (SA) and lenticular (LA) galaxies of the (*r*) and (*rs*) varieties. Sources of photographs (see code in Table 1B): (*a*) NGC 1553 (II, b, D, RS); (*b*) NGC 7702 (II, b, D, GV); (*c*) NGC 4736, inner ring and nuclear region only (IV, c, EGC [*U* band], PG); (*d*) NGC 4736, outer disk structure (IV, c, EGC, PG); (*e*) NGC 4501 (VI, a, D, FB); (*f*) NGC 5364 (VI, c, D, GV); (*g*) NGC 7531, inner ring and nuclear region only (III, c, D, KF); (*h*) NGC 7531, outer disk structure (II, b, D, GV).

Note 1.—The inner ring of NGC 1553 does not show well in the illustration; however, the ring is clearly visible on the original print as a distinct enhancement near the outer edge of the lens.

Note 2.—Unless otherwise stated, all photographs in this Figure and in Figures 2 and 3 (Plates 14 and 15) are from blue (B) band plates.

© American Astronomical Society • Provided by the NASA Astrophysics Data System

1980ApJS...44..451D

PLATE 14

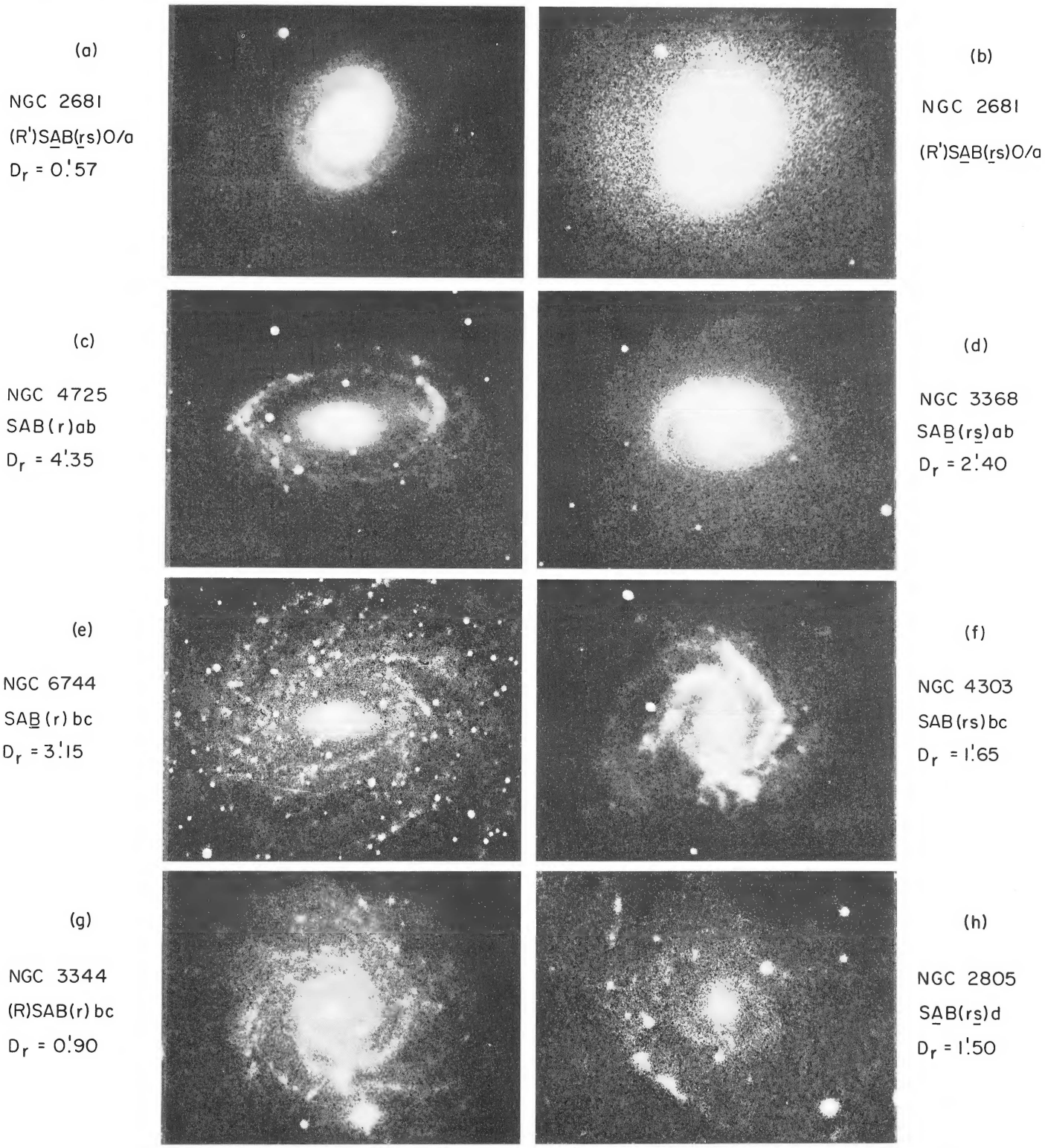

FIG. 2.—Examples of intermediate barred spiral (SAB) galaxies of the (*r*) and (*rs*) varieties. Sources of photographs: (*a*) NGC 2681, inner pseudoring and nuclear region only (VI, c, D, GV); (*b*) NGC 2681, outer envelope (VII, c, IT, JW); (*c*) NGC 4725 has anomalous tightly wound single arm outside ring (IV, c, EGC, RB); (*d*) NGC 3368 (IV, *c*, IT, JW); (*e*) NGC 6744 (II, b, D, GV); (*f*) NGC 4303 has broken hexagonal inner ring (VI, a, D, GV); (*g*) NGC 3344 (IV, c, IT, JW); (*h*) NGC 2805, one of latest stages showing traces of an inner ring (IV, c, IT, JW).

© American Astronomical Society • Provided by the NASA Astrophysics Data System

1980ApJS...44..451D

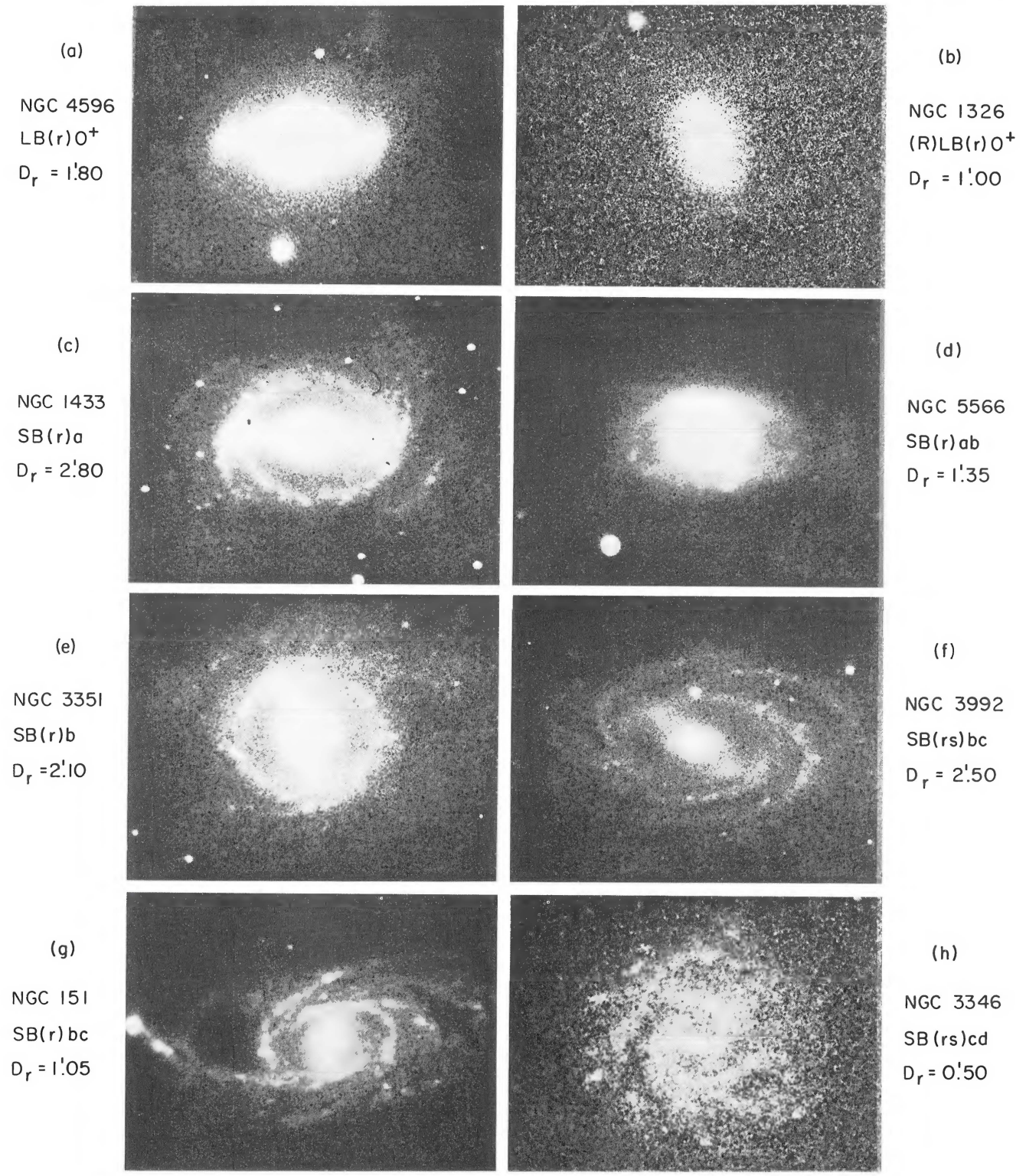

FIG. 3.—Examples of barred spiral (SB) and lenticular (LB) galaxies of the (*r*) and (*rs*) varieties. Sources of photographs: (*a*) NGC 4596 has typical blobs where faint ring intersects bar (VII, c, IT, JW); (*b*) NGC 1326 has faint outer ring and inner (*r*) or (*rs*) structure (I, b, D, GV); (*c*) NGC 1433 has elongated ring in face on disk (II, b, D, GV); (*d*) NGC 5566, inner lens and ring only (IV, c, EGC, PG); (*e*) NGC 3351 has apparent circular ring in inclined disk (IV, c, IT, JW); (*f*) NGC 3992 (V, c, IT, JW); (*g*) NGC 151 (VI, c, IT, JW); (*h*) NGC 3346 (V, c, IT, JW).

© American Astronomical Society • Provided by the NASA Astrophysics Data System

1980ApJS...44..451D

TABLE 1A

EXAMPLES OF NGC GALAXIES WITH INNER RINGS[a]

	TYPES	LENTICULARS	S0/a, Sa, Sab	Sb, Sbc, Sc	Scd, Sd, Sdm
Family	Variety	−3 to −1	0–2	3–5	6–8
A	(r)	1553, 4429	4736, 7217	488, 6753	4571 ...
		7702 ...	... ...	7531 ...	... ...
	(rs)	524, 7457	2855, 4501,	1068, 5055	... ...
		... ...	4750 ...	5364 ...	... ...
AB	(r)	3081, 3419	4725, 4941	3344, 5985	1179, 5967
		... ...	5448, 5728	6384, 6744	... ...
	(rs)	2962, 3489	2681, 3368,	4303, 4536	2805, 5068,
		... ...	7098 ...	... ...	6946
B	(r)	1326, 4340,	1433, 1512	151, 3351,	1493 ...
		4371, 4596	4274, 5566	5850 ...	... ...
	(rs)	936, 2983	4643, 5101	3059, 3992,	3346 ...
		... ...	... ...	4548, 5792	IC 5201 ...

[a]Italic numbers are designations for galaxies illustrated in Figure 1, 2, or 3.

TABLE 1B

CODES OF PHOTOGRAPHS

Telescope	I = Mount Stromlo 0.76 m; II = Mount Stromlo 1.9 m; III = Siding Spring 1.0 m; IV = McDonald 0.76 m; V = McDonald 0.91 m; VI = McDonald 2.1 m; VII = McDonald 2.7 m.
Focus.....	a = prime; b = Newton; c = Cassegrain
Camera ...	EGC = electronographic; IT = image tube; D = direct
Observer ..	FB = F. Bertola; RB = R. Buta; PG = P. Griboval; RS = R. Shobbrook; GV = G. de Vaucouleurs; JW = J. Wray

plete ring affects a characteristic hexagonal shape. Examples are given in Table 1 and illustrated in Figure 2. In principle and by definition, spirals of the (*s*) variety do not exhibit inner ring structures, although occasionally the spiral arm pattern may mimic circular or elliptical rings which are described as pseudo-(*r*) in the *notes* to RC1 and RC2 (de Vaucouleurs and de Vaucouleurs 1964; de Vaucouleurs, de Vaucouleurs, and Corwin 1976). Overall, nearly 50% of all L and S galaxies for which the variety is specified in RC2 have (*r*) or (*rs*) structures.

Frequently the main bodies of galaxies of the (*r*) and (*rs*)—and occasionally even (*s*)—varieties are surrounded by a fainter, larger, outer ring structure, denoted (*R*), of which NGC 1068, 1291 and 4736 offer the best known examples (see *Hubble Atlas*, Sandage [1961] page 16; de Vaucouleurs [1956*a*, *b*, 1959*c*] Figs. 12, 16, 22, 29, and 49; Kormendy [1979], Figs. 9, 10, 12, and 13). Often the outer (*R*) is made up of two or more tightly coiled spiral arms; NGC 1291 (de Vaucouleurs 1975*a*) is a good example. Sometimes the outer arms of a spiral galaxy (of any variety) form an incomplete or broken pseudo-outer ring, denoted (*R*′)—or *P* in RC2 notation. In the largest examples 21 cm line studies show that this outer (*R*) or (*R*′) structure is also the locus of a ring-like concentration of neutral hydrogen; examples are NGC 1291 (Mebold *et al.* 1979), NGC 4151 (Bosma, Ekers, and Lequeux 1977), and NGC 4736 (Bosma, van der Hulst, and Sullivan 1977).[1] Because these outer rings are much fainter than the inner rings they were often overlooked until the 1950s.[2]

The small-scale high-contrast images on sky-limited Schmidt plates, such as the POSS, ESO-B and UKSTU plates, are best to detect the large, faint outer (*R*) rings, but are often useless for the study of the smaller inner (*r*) rings which are visible on large-scale Cassegrain focus, short-exposure photographs. In the present study we will only consider the well-documented inner (*r*) and (*rs*) structures, leaving the (*R*) and (*R*′) structures for separate future analysis.

Theories of the formation of inner and outer ring structures in galaxies have been proposed by Randers

[1]These formations should not be confused with the bright annular component (B) of the so-called ring galaxies which is probably an unrelated phenomenon, possibly resulting from collisions of galaxies with intergalactic gas clouds or with other galaxies (Freeman and de Vaucouleurs 1974; Theys and Spiegel 1976; Lynds and Toomre 1976), or perhaps from internal explosive events (Vorontsov-Velyaminov 1976; Dostal and Metlov 1978).

[2]The inner rings which are often bright enough to be seen visually through a large reflector were first depicted by Lord Rosse and his collaborators (Parsons 1926) and by Lassell (1866) whose striking sketch of the center of NGC 4736 was reproduced by Flammarion (1920). While the inner rings of the SB types were formally recognized as characteristic of the "Φ-type" by Curtis (1918), the first description of a typical outer ring structure (that of NGC 1291) was published by Perrine (1922), although it was already visible on a Franklin-Adams chart (number 29) of 1910.

© American Astronomical Society • Provided by the NASA Astrophysics Data System

1980ApJS...44..451D

(1940) who explored hydrodynamical concepts and by Freeman (de Vaucouleurs and Freeman 1972) who developed analytical and numerical particle-trapping models. It has also been suggested by several authors (see, e.g., Schommer and Sullivan 1976) that the inner and outer rings may be located at or near the inner and outer Lindblad resonances, but the rotation velocity curve has been determined with sufficient detail in too few galaxies for a critical test of this suggestion that would establish whether this coincidence is an accident or the rule. Often the inner ring is too small to be resolved at 21 cm (although the VLA will soon change this) and the outer ring is too faint for detection by optical spectrographs. Reference is made to an excellent study of the inner ring of NGC 4736 by van der Kruit (1976) for details of the velocity field in a typical example.

The idea of using the well-defined diameters of inner rings in L and S galaxies of the (r) and (rs) types as *metric* distance indicators was first proposed by one of us more than 20 years ago, and a preliminary application was made to the derivation of the relative distances of several groups of southern galaxies observed with the Reynolds reflector at Mount Stromlo (de Vaucouleurs 1956*b*, 1957*a*). The hope, of course, was that the diameter defined by the ridge line of the brightness distribution, being an easily measured metric length, would be essentially free of the systematic errors which plague the concept of isophotal (and, worse, photographic) diameters of galaxies (Holmberg 1946; de Vaucouleurs 1959*a*, *b*).

In the original concept all rings were assumed to have the same average linear diameter irrespective of family (SA versus SB) or stage (a,b,c...) along the Hubble sequence. However, it soon became clear that the inner rings in ordinary spirals (SA) are much smaller than in barred spirals (SB) both in terms of absolute linear diameter and also relative to the outer isophotal diameter D_o of a galaxy. This was illustrated qualitatively by the revision of the diagram depicting a cross section of the classification volume (Fig. 4 [Plate 16]) (compare the original version of Fig. 1 in de Vaucouleurs [1957*b*], Plate 2A and in de Vaucouleurs [1959*c*], Plate 1 with the revised version in de Vaucouleurs [1970], Fig. 1 and in Sandage [1975], Fig. 5) and quantitatively by a tabulation of mean linear diameters in galaxies of different types (de Vaucouleurs 1970, Table 2). With allowance for the recent revision of the distance scale (de Vaucouleurs 1979*a*, *b*), the inner rings of SA spirals average approximately 3.5 kpc in diameter against 7 kpc in SB spirals with intermediate values in the weak-bar transition type SAB.[3]

[3]It should be kept in mind that the very small ring structures occasionally seen in galactic nuclei (e.g., in NGC 1097, 4314, 4321, 5248) and discussed among others by Lynds, Furenlid, and Rubin (1973) and Benedict *et al.* (1977) are not considered here and have little or no bearing on the (r) designation.

It became also evident that ring diameters scale up in proportion to the overall diameter of a galaxy measured either by its isophotal diameter D_o (in RC2 notation) or by its effective (metric) diameter D_e; that is, all other things being equal, intrinsically large galaxies have larger rings than small galaxies. It follows that in order to make the best possible use of ring diameters as distance indicators some distance-independent index of absolute diameter (or luminosity) such as luminosity *class* LC (van den Bergh 1960*a*, *b*) or better the corrected luminosity *index* Λ_c (de Vaucouleurs 1977, 1979*a*; de Vaucouleurs, de Vaucouleurs, and Corwin 1978) is needed.

Between 1953 and 1963 the senior author reclassified a large number of galaxies in the revised classification system and measured the diameters of inner and outer rings (and of lenses) on large-scale reflector plates in more than 500 galaxies. The best 1500 of the revised types were published separately (de Vaucouleurs 1963*a*), while the diameter data appeared mainly in the *notes* to RC1. This material was collated and transferred to punched cards in 1966–1967 by P. Schultz, who made a first statistical study of the data. The catalog, with revisions and additions, was recently published (de Vaucouleurs and Buta 1980); some results from this study were presented in 1969 at the IAU Symposium No. 38 held in Basel (de Vaucouleurs 1970). However, in the absence of reliable distances to most of the galaxies at the time, this first study had to depend on tentative estimates based on provisional distances to galaxy groups or on the conventional assumption of a linear-isotropic velocity-distance relation, even though it was already clear that this assumption is at best only a first approximation (see de Vaucouleurs 1958, 1966; de Vaucouleurs and Peters 1968). Furthermore, selection effects in an (essentially) magnitude-limited sample and other calibration errors introduced severe nonlinearity problems in the derived distance scale (de Vaucouleurs 1972, 1975*b*). Until these problems were sorted out little progress could be made with the absolute calibration of ring structures as distance indicators.

There are several reasons why it is now timely to reinvestigate the statistical properties of the (r) and (rs) structures in galaxies and, in particular, those which have a direct bearing on their uses as metric distance indicators:

(i) New data of much improved quality are now available on types, diameters, magnitudes, colors, H I fluxes, and redshifts for a large number of bright galaxies listed in RC2.

(ii) The recent progress in the construction of an extragalactic distance scale free of gross calibration errors and nonlinearity (de Vaucouleurs 1979*a*, *b*; Wray and de Vaucouleurs 1980) allows distances independent of any assumption on the redshift law to be estimated for several hundred spiral galaxies with individual mean errors less than 20%.

© American Astronomical Society • Provided by the NASA Astrophysics Data System

1980ApJS...44..451D

PLATE 16

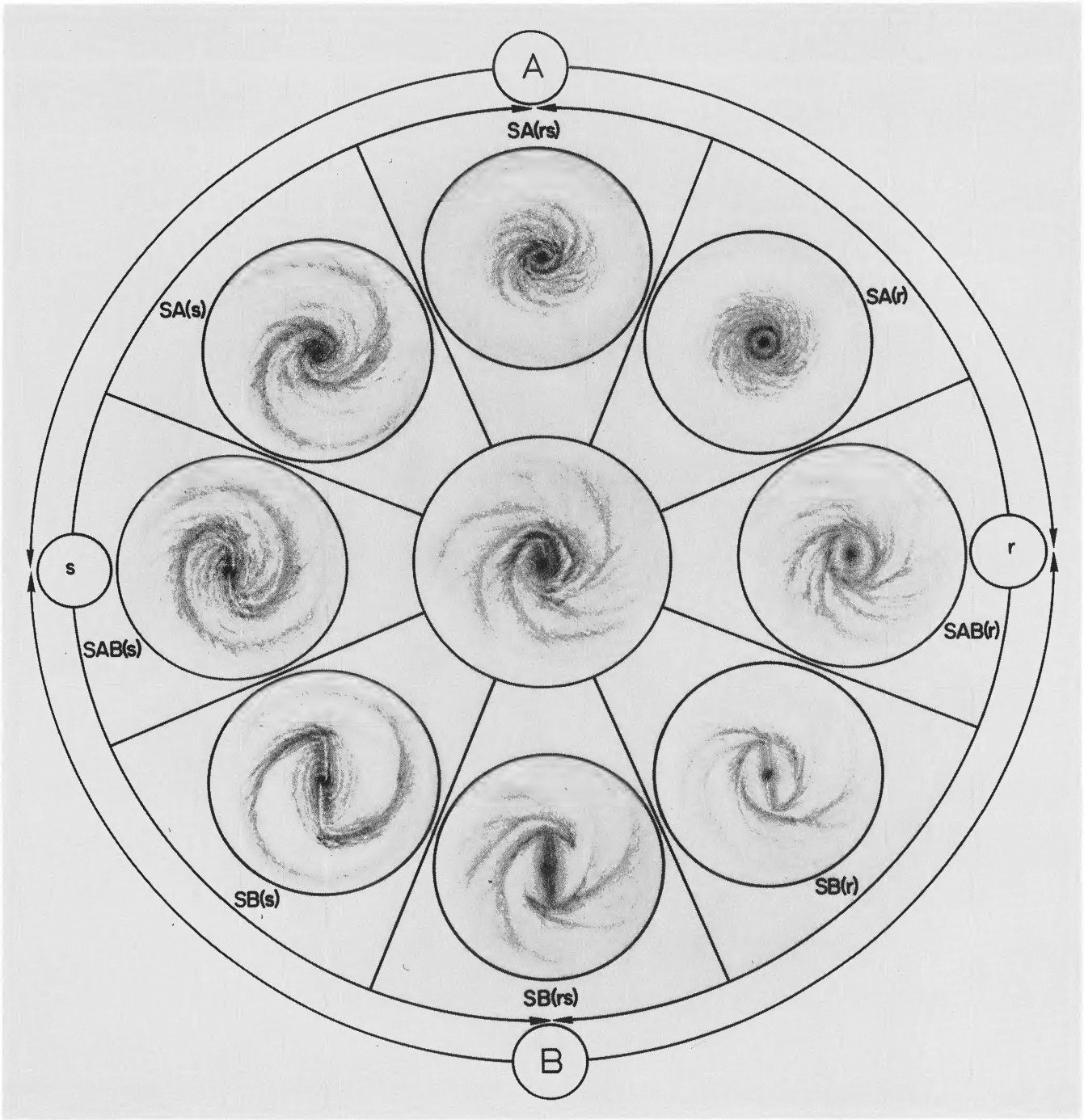

FIG. 4.—Cross section of the revised Hubble System near stage Sb, illustrating the arrangement of families and varieties in the classification volume. All galaxies are rectified to a face-on presentation with approximately consistent scales; illustrated prototypes are SA(*rs*): NGC 1068, SA(*r*): NGC 7217, SAB(*r*): NGC 6744, SB(*r*): NGC 1433, SB(*rs*): NGC 1073 and 3359.

DE VAUCOULEURS AND BUTA (*see* page 453)

© American Astronomical Society • Provided by the NASA Astrophysics Data System

1980ApJS...44..451D

(iii) The work of Sandage and Visvanathan (1978) and Visvanathan and Griersmith (1979) on the color-magnitude relation for early-type galaxies, and of Michard (1979*a*, *b*) on the diameter-magnitude-color relations for E and L galaxies will soon provide fairly reliable distances to several hundred lenticular galaxies with individual mean errors less than 30% (a comparison of various distance scales and their reduction to a uniform system will be reported later).

(iv) A recent resurvey of 121 bright SB galaxies by Kormendy (1979) giving new data on ring and lens diameters allows a comparison of ring (and lens) diameters for 43 objects in common and an objective assessment of external precision for diameter and ellipticity data.

(v) A large number of additional objects south of $\delta = -17°$ are being classified by Corwin on UK 125 cm Schmidt telescope plates (Corwin, de Vaucouleurs, and de Vaucouleurs 1977, 1978) which will greatly strengthen and enlarge the material on types, luminosities, and diameters, particularly of ring structures, in the southern hemisphere.

(vi) The resurvey of southern Shapley-Ames galaxies by Sandage and collaborators (Dressler and Sandage 1978; Sandage and Brucato 1979) with the 1.0 and 2.5 m reflectors at Las Campanas will also strengthen the classification (type, luminosity class) of southern objects.

In the present paper we will study the systematics of inner ring structures, mainly in dimensionless units, versus classification parameters, i.e., galaxy class (L versus S), family (A versus B), variety (*r* versus *rs*) and stage (L^-–Sm, or $T = -3 - +9$ in RC2 notation), and in relation to quantitative parameters such as galaxy diameter (metric or isophotal), inclination (or axis ratio), absolute magnitude (or luminosity index), etc. In a second paper the results of the present study will be applied to the absolute calibration of ring diameters which will then be used to derive distances of several hundred spiral and lenticular galaxies of the (*r*) and (*rs*) varieties.

Our basic material is the card catalog of 532 galaxies prepared by P. Schultz, of which 423 have ring diameters (*r*) and (*rs*) measured by one of us (G. V.) mainly on large-scale reflector plates. The classifications were updated to take into account revised types given in RC2 and we have also considered the finer classifications (such as $\underline{AB}$ or $\underline{rs}$, rather than just AB or *rs*) given in de Vaucouleurs (1963*a*). It turns out that these refinements (although neglected for simplicity in RC1 and RC2) are significant and can improve the analysis of the (*r*), (*rs*) diameters.

We present in § II revised tables of the frequency distributions of (*r*) and (*rs*) structures among galaxies of different morphological types and attempt to allow for selection effects depending on apparent diameter, axis ratio, etc. to derive true (space) frequencies from the apparent (catalog) frequencies.

In § III we compare the independent measurements of major axis diameters and axis ratios by Kormendy (1979) with ours to evaluate measuring errors and we compare also the axis ratios of the galaxies ($\log R_{25}$ as listed in RC2) and of the rings ($\log D_r/d_r$) to evaluate inclination effects and true ellipticities.

In § IV we compare the diameters of the rings and of the parent galaxies (D_o, A_e as listed in RC2) and study the dependence of the ratios (X, Y) on type, family, variety and luminosity class. In particular we demonstrate that the ratios $X = \log D_o/D_r$ and $Y = \log A_e/D_r$ can be used to quantify the concept of family or strength of the bar.

Although our present material is more extensive than in other studies we do not claim or attempt to present an exhaustive study of the properties of inner ring structures in galaxies and we purposely neglect second-order effects (e.g., possible ellipticity of the rings in SB types), which will be considered later in greater detail (by R. B.) in a special study of a selected sample as part of a dissertation research project. Our immediate and restricted purpose here is to discuss some statistical properties of the rings which need to be known for their proper use as distance indicators.

II. RELATIVE FREQUENCIES OF INNER RING STRUCTURES IN GALAXIES

a) *General Statistics*

A total of 2399 galaxies are classified as spirals in RC2; 632 are classified as lenticular galaxies. Of these objects, 1559 of the spirals and 186 of the lenticulars are assigned to one of the varieties (*r*) or (*s*), or to the mixed variety (*rs*), as defined in the revised Hubble system. Table 2A summarizes the raw statistics of the distribution of these varieties over the total of 1745 galaxies, without regard to classification weight, diameter, axis ratio, family, or stage. It is seen that the pure ring variety (*r*) comprises a substantial though small fraction (21%) of the sample while the pure (*s*) variety comprises nearly half the sample. This dominance of the (*s*) variety over the (*r*) variety was first noted by de Vaucouleurs (1963*a*) in a sample of 1500 well-classified galaxies, and it occurs mainly in the spirals. In the present sample, $N(s) = 2.75\ N(r)$ for the spirals, and hence there is a substantial imbalance. No such imbalance is apparently present among the lenticulars, but their classification according to variety is less certain, particularly for inclined objects (see § II*c*).

Because the visibility of rings evidently depends on the number of resolution elements in the image, and thus on apparent diameter, a better idea of the general

© American Astronomical Society • Provided by the NASA Astrophysics Data System

1980ApJS...44..451D

TABLE 2

SOME GENERAL STATISTICS OF VARIETIES AMONG RC2 GALAXIES

Type	$N(r)$	$N(rs)$	$N(s)$	N.A.	Totals
			All RC2 Galaxies		
S	284	493	782	840	2399
L	89	23	74	446	632
Totals ...	373	516	856	1286	3031
f(%)[a]	21.4	29.6	49.0	42.4	...
			$W_T \geq 2.6$		
S	173	328	452	79	1032
L	67	17	55	131	270
Totals ...	240	345	507	210	1302
f(%)	22.0	31.6	46.4	16.1	...
			$D_0 > 2'.0$, $\log R_{25} \leq 0.2$		
S	123	217	198	73	611
L	32	13	35	72	152
Totals ...	155	230	233	145	763
f(%)	25.1	37.2	37.7	19.0	...
			$D_0 > 2'.0$, $\log R_{25} > 0.2$		
S	59	119	273	173	624
L	26	4	15	76	121
Totals ...	85	123	288	249	745
f(%)	17.1	24.8	58.1	33.4	...

[a] The percentage of varieties are based only on those galaxies having varieties. The percentages of N.A. (no variety given) is based on the total sample.

relative frequency of inner rings may be obtained by restricting the statistics to galaxies of high classification weight W_T (as defined in RC2), or which have a diameter larger than some nominal limit and a small inclination. The relative frequencies of the three varieties over all spiral and lenticular galaxies having a classification weight $W_T \geq 2.6$ (the mean weight in the RC2), are summarized in Table 2B. Note that in this case only 16% of the total 1302 objects are without varieties (versus 42% for all W_T), and hence the relative frequencies derived from this sample should be more representative of the true frequencies. Much the same distribution as in Table 2A results, however, with 22% of the galaxies being of the pure (r) variety, and $N(s) = 2.61\ N(r)$ for the spirals.

A similar analysis restricted to the sample of galaxies having $D_0 > 2'.0$ (the median corrected diameter in RC2) and $\log R_{25} \leq 0.2$ (the median axis ratio in RC2) is presented in Table 2C. Rings now comprise 25% of the sample with $N(s) = 1.6\ N(r)$, which confirms that the apparent dominance of the (s) variety is largely an artifact due to inadequate resolution in the smaller or more inclined objects or both. Note that of 763 galaxies satisfying these restrictions, 19% were not assigned varieties in the RC2. The analysis in Table 2D shows for comparison the statistics for galaxies having $\log R_{25} > 0.20$, and comprises a nearly equally large sample (745 objects); but now 33% have no variety given, and the relative frequency of the (r) variety drops to 17% with $N(s) = 4.6\ N(r)$ for the spirals. Evidently it is more difficult to detect rings in strongly inclined objects, and the high percentage of objects without varieties in this case is not surprising. More details on the dependence of the relative frequencies on $\log R_{25}$ is given in § II*c*.

b) *Dependence of the Relative Frequencies on Family and Stage*

We will now show that the distribution of varieties (r, rs, s) is different among the three families (A, AB, B), and is strongly dependent on stage as was already indicated by de Vaucouleurs (1963*a*). We will treat the spirals and lenticulars separately, since as the numbers in Tables 2A–2D indicate, the distribution of varieties is different between these two major classes.

Tables 3A and 3B give the relative frequencies of varieties among RC2 spiral and lenticular galaxies, separated by family, and according to weight, diameter,

© American Astronomical Society • Provided by the NASA Astrophysics Data System

1980ApJS...44..451D

TABLE 3A

RELATIVE FREQUENCIES OF VARIETIES AMONG RC2 SPIRALS

Restriction	SA(r)	SA(rs)	SA(s)	N	SAB(r)	SAB(rs)	SAB(s)	N	SB(r)	SB(rs)	SB(s)	N
All RC2 spirals (%)....	14.9	25.8	59.3	396	18.1	45.4	36.5	491	20.2	25.0	54.8	672
$W_T \geq 2.6$.....	13.7	22.0	64.3	291	18.6	53.8	27.6	301	21.1	28.3	50.6	360
$W_T < 2.6$.....	18.4	35.7	45.9	98	17.7	31.5	50.8	181	19.4	21.1	59.5	294
$D_0 > 2'.0$, $\log R_{25} \leq 0.2$.	15.5	27.1	57.4	129	20.5	54.6	24.9	205	29.9	34.3	35.8	204
$D_0 > 2'.0$, $\log R_{25} > 0.2$.	7.5	21.8	70.7	147	13.8	41.4	44.8	116	16.1	21.0	62.9	186
$D_0 \leq 2'.0$, $\log R_{25} \leq 0.2$.	18.1	33.7	48.2	83	18.7	35.8	45.5	123	20.6	24.1	55.3	170
$D_0 \leq 2'.0$, $\log R_{25} > 0.2$.	40.0	13.3	46.7	30	18.4	39.5	42.1	38	7.4	14.9	77.7	94
$V_0 \leq 2400$, $\log R_{25} \leq 0.2$	10.8	24.3	64.9	74	10.7	63.1	26.2	103	21.0	28.6	50.5	105
$V_0 \leq 2400$, $\log R_{25} > 0.2$	6.1	20.7	73.2	82	10.0	48.0	42.0	50	11.7	16.9	71.4	77
$V_0 > 2400$, $\log R_{25} \leq 0.2$	20.8	36.4	42.9	77	18.3	41.3	40.4	104	25.2	30.8	43.9	107
$V_0 > 2400$, $\log R_{25} > 0.2$	24.0	4.0	72.0	25	11.1	51.9	37.0	27	17.6	21.6	60.8	51

TABLE 3B

RELATIVE FREQUENCIES OF VARIETIES AMONG RC2 LENTICULARS

Restriction	LA(r)	LA(rs)	LA(s)	N	LAB(r)	LAB(rs)	LAB(s)	N	LB(r)	LB(rs)	LB(s)	N
All RC2 Lenticulars (%) .	57.0	6.3	36.7	79	50.0	15.0	35.0	40	35.8	17.9	46.3	67
$W_T \geq 2.6$.....	55.0	8.3	36.7	60	53.8	11.5	34.6	26	37.3	17.6	45.1	51
$W_T < 2.6$.....	61.1	0.0	38.9	18	41.7	16.7	41.7	12	33.3	20.0	46.7	15
$D_0 > 2'.0$, $\log R_{25} \leq 0.2$...	42.9	8.6	48.6	35	43.8	18.8	37.5	16	32.1	25.0	42.9	28
$D_0 > 2'.0$, $\log R_{25} > 0.2$...	81.0	4.8	14.3	21	60.0	20.0	20.0	5	33.3	11.1	55.6	18
$D_0 \leq 2'.0$, $\log R_{25} \leq 0.2$...	50.0	0.0	50.0	16	45.5	9.1	45.5	11	50.0	16.7	33.3	18
$D_0 \leq 2'.0$, $\log R_{25} > 0.2$...	66.7	16.7	16.7	6	66.7	0.0	33.3	6	0.0	0.0	100.0	2
$V_0 \leq 2400$, $\log R_{25} \leq 0.2$..	42.1	10.5	47.4	19	50.0	20.0	30.0	10[a]	27.3	27.3	45.5	22
$V_0 \leq 2400$, $\log R_{25} > 0.2$..	83.3	8.3	8.3	12					25.0	8.3	66.7	12
$V_0 > 2400$, $\log R_{25} \leq 0.2$..	40.0	5.0	55.0	20	40.0	10.0	50.0	10[a]	30.0	20.0	50.0	10[a]
$V_0 > 2400$, $\log R_{25} > 0.2$..	50.0	12.5	37.5	8								

[a] Because of the small numbers involved, the $\log R_{25}$ restriction had to be relaxed. In each case, only the highest $\log R_{25}$ was rejected.

axis ratio, and radial velocity. Among the larger SA spirals, the relative frequency $f(r)$ of the (r) variety decreases from 15.5% for objects of low inclination to only 7.5% for those of high inclination, reflecting again the difficulty of detecting rings in highly tilted spirals. Similarly, among the SAB galaxies, the (rs) variety dominates substantially among galaxies of high weight, but this trend is largely lost among galaxies of low weight. Perhaps the most extreme case is that of the LA galaxies. Table 3B shows that among the larger LA galaxies $f(r)$ *increases* from 43% at $\log R_{25} \leq 0.2$ to 81% for $\log R_{25} > 0.2$, a trend unexpectedly opposite to that in spirals. This high frequency of (r) classification among the highly inclined lenticulars is probably an artifact, for very often the presence of a ring is only inferred from dust or intensity distribution in the edge-on view of the lens. This peculiar result is further discussed in § II*c*.

Because the most reliable classifications are those for galaxies of high weight, large diameter, low inclination, or low radial velocity, we believe the frequencies calculated in these cases to be more nearly representative of the true frequencies of the varieties. However, even these restrictions may not be sufficient since the weight restriction does not necessarily exclude highly inclined objects, and the velocity or $\log R_{25}$ restriction does not necessarily exclude objects of small angular diameter. Restricting our attention, then, to the relative frequencies among the larger, more nearly face-on galaxies, we find that among the spirals the pure ring variety is most abundant in the SB family, where $f(r) = 30\%$, and is least abundant in the SA family, where $f(r) = 15.5\%$. In both of these cases the (s) variety dominates the (r) variety but the imbalance is substantially different: $N(s) = 3.7\ N(r)$ for the SA family and only $1.2\ N(r)$ for the SB family. Among the SAB galaxies, the (s) variety again dominates the (r) variety, but it does not have the highest relative frequency. Instead, the classification SAB (rs) is dominant, comprising 55% of the SAB galaxies with reasonably trustworthy classifications.

It is not clear why the (rs) variety should be especially important among the SAB galaxies. Variety is actually a continuous parameter; it can be subdivided further than we have yet considered, for example, as (r), ($\underline{r}s$), (rs), ($r\underline{s}$), (s) (de Vaucouleurs 1963*a*), where the underscores indicate the dominant form. This implies that there is a large range of forms that could be classified (rs) among galaxies, with the pure varieties (r) and (s) being the endpoints of a continuum. If the dominance of the (rs) variety among SAB galaxies is real, then this implies an intimate connection between

© American Astronomical Society • Provided by the NASA Astrophysics Data System

1980ApJS...44..451D

weak bars (AB) and broken pseudo rings (*rs*), an observation which may have dynamical significance. However, one must be careful before considering such an interpretation because SAB(*rs*) is the principal hybrid galaxy type: in the three-dimensional classification volume of the revised Hubble system (Fig. 4), it lies in the center of the continuum of forms, and all the "purer" types, such as SB(*r*), SA(*s*), etc., merge into this common section of the volume. It may be that the high frequency of SAB(*rs*) galaxies is merely the result of assigning a larger fraction of the classification volume to the central hybrid form. In the absence of quantitative classification criteria, results of statistics based on subjective classification schemes must be treated with caution.

Among the lenticular galaxies the relative frequencies of varieties are noticeably different from those of the spirals. If we restrict our attention once again to the large objects of low inclination, then we find that the (*r*) variety has the highest relative frequency among the LA and LAB galaxies, where $f(r) \approx 43\%$ in each case, compared to $f(r) = 32\%$ for the LB galaxies. However, these numbers are less significant than those for the spirals, because of the relatively small numbers of objects involved, and because the classification of lenticular galaxies is somewhat difficult [the features which distinguish (*r*) from (*rs*) and (*s*) forms being only weakly differentiated in these early-type galaxies, very high-quality plate material is usually necessary to classify them accurately]. For example, in all three families, particularly LA, there is a deficiency of the (*rs*) variety. De Vaucouleurs (1963*a*) has noted that this deficiency is not likely to be real, but probably results from difficulty of classification. In general, for the lenticular galaxies the relative frequencies of the (*r*) and (*s*) varieties are roughly equal, although there is still a slight dominance of the (*s*) variety over (*r*) for the LB galaxies.

The relative frequencies of varieties also show a pronounced dependence on stage *T* along the Hubble sequence. This is illustrated in Figure 5 for the (*r*) and (*rs*) varieties only, without regard to family, and sub-

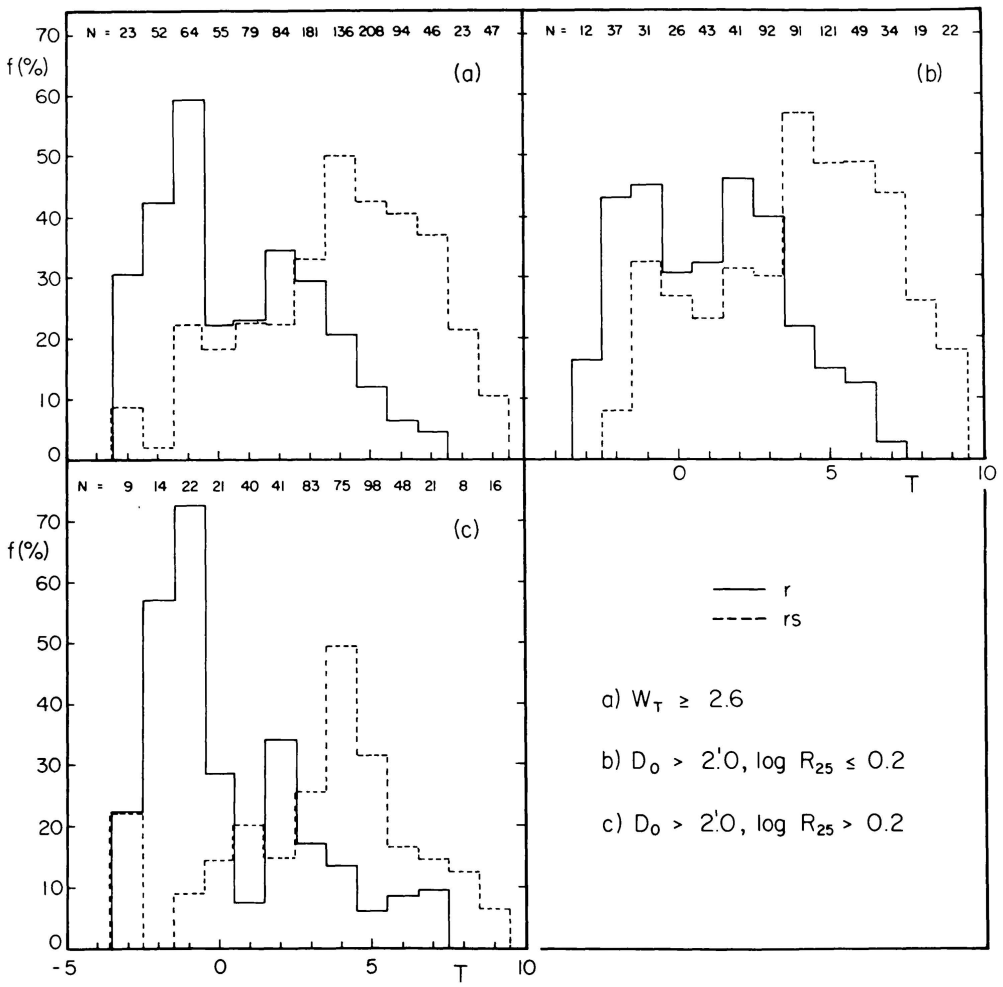

FIG. 5.—Histograms of the relative frequency of the (*r*) and (*rs*) varieties as a function of numerical stage *T* along the revised Hubble sequence, without regard to family. The statistics are based entirely on RC2 data and are limited only to galaxies satisfying the restrictions indicated in the lower right box of the figure. The numbers of objects *N* at each type included in the statistics are shown at the top of each box.

© American Astronomical Society • Provided by the NASA Astrophysics Data System

1980ApJS...44..451D

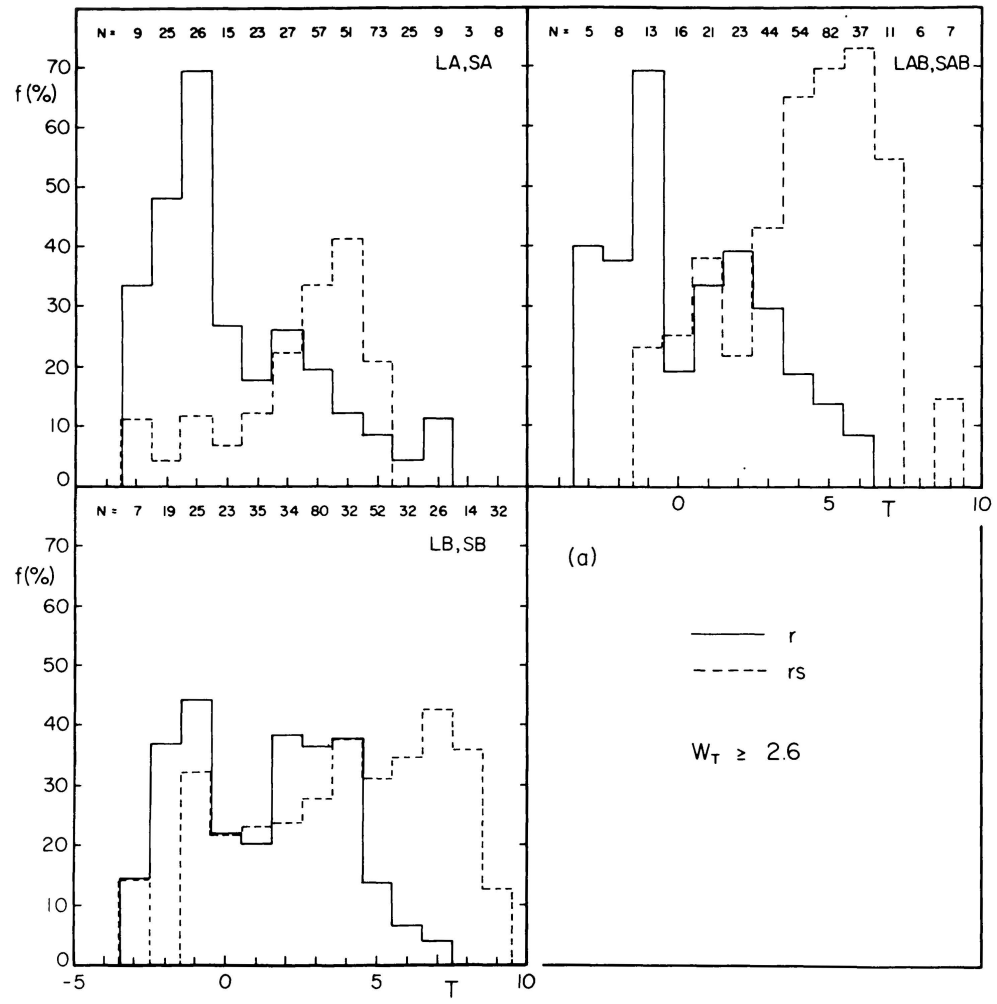

FIG. 6a

FIG. 6.—Histograms of the relative frequency of the (*r*) and (*rs*) varieties as a function of numerical stage *T* along the revised Hubble sequence, separated by family A, AB, and B. The statistics are restricted (*a*) according to weight, and (*b*) according to diameter and axis ratio.

ject to restrictions with regard to weight (Fig. 5*a*) and diameter and axis ratio (Figs. 5*b* and *c*). The relative frequency of the (*r*) variety has two probable maxima near stages $T=-1$ ($S0^+$) and $T=2$ (Sab), and the sizes of the maxima are sensitive to the indicated restrictions. As suggested by de Vaucouleurs (1963*a*), the relative frequency function of inner rings appears to be bimodal and could be the sum of two possibly unrelated roughly gaussian components (one for the spiral and another for the lenticular galaxies). In any case, rings are very common among late lenticular and early-to-intermediate stage spiral galaxies, while the ring phenomenon evidently weakens considerably (or becomes more difficult to detect) among the late spiral stages and the earliest lenticular stage. (Note, however, that some of the points in Fig. 5 are not very significant due to the small size of the sample).

It is interesting to note that the peak at stage $T=-1$ is considerably smaller when the statistics are restricted to $D_o > 2.0$, $\log R_{25} \leq 0.2$ than when they are restricted by weight or to $D_o > 2.0$, $\log R_{25} > 0.2$. Since the weight restriction does not completely exclude highly inclined objects, we see that the value of $f(r)$ at $T=-1$ in Figure 5*a* lies between the corresponding values in Figures 5*b* and 5*c*, so that highly inclined lenticular galaxies are partly responsible for the large peak in Figure 5*a*. If the frequency distribution in Figure 5*b* is taken to be more representative of the true distribution, then the ring frequency $f(r) \approx 45\%$ among $T=-1$ and -2 galaxies is nearly identical to that at $T=2$.

The dependence on family of the relative frequency distribution function of the (*r*) variety (restricted by weight and $D_o > 2.0$, $\log R_{25} \leq 0.2$) is shown in Figures 6*a* and 6*b*. Although the samples are even smaller than

© American Astronomical Society • Provided by the NASA Astrophysics Data System

1980ApJS...44..451D

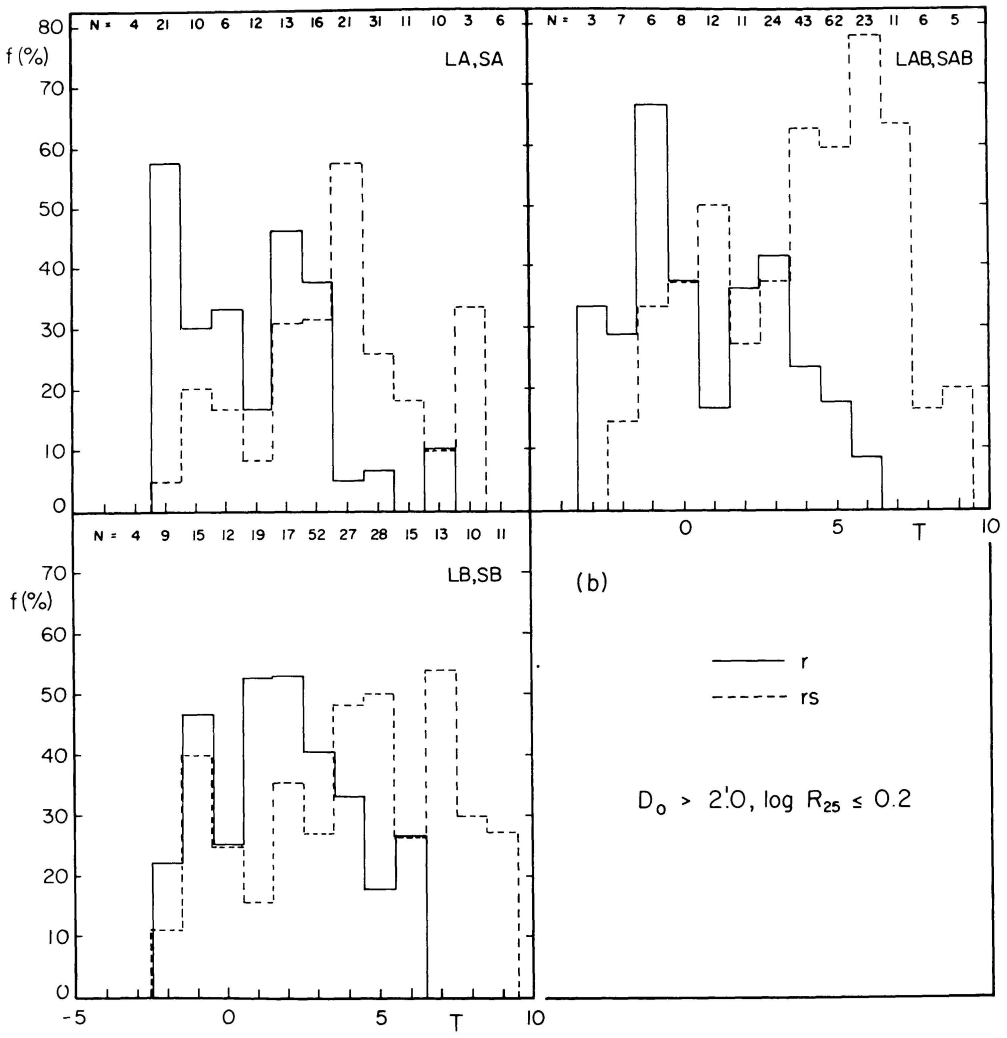

FIG. 6b

in Figures 5*a* and 5*b*, the locations of the peaks in Figure 6 do not differ significantly (not more than ± 1 T unit) from their positions in Figure 5. This strengthens the significance of the distributions illustrated in Figure 5, which apply to galaxies of all families.

The distribution of the mixed variety (*rs*) is also illustrated in Figure 5. All three graphs indicate a substantial peak at $T=4$ among the spirals, with only a marginally significant peak among the lenticular galaxies at $T=-1$ in Figure 5*b*. But in this case the relative distributions are significantly different for different families, as shown in Figures 6*a* and 6*b*. For example, $f(rs)$ peaks at $T=6$ among the SAB galaxies in both graphs while for the SA galaxies it peaks at $T=4$. For SB galaxies the distribution is more erratic across the spiral sequence, but in this case $f(rs)$ is larger in the $T=4$–7 range also. We conclude that whereas the (*r*) variety is most common among the early-to-mid spiral stages, the (*rs*) variety appears to be more common (or more easily recognized) among the late spirals.

c) *Relative Frequencies of Varieties as Functions of Weight, Diameter, and Axis Ratio*

The relative frequencies of the (*r*), (*rs*) and (*s*) varieties as functions of weight, $\log D_0$ and $\log R_{25}$ were studied by dividing the total samples into several bins of nearly equal numbers of objects. This was done to study in detail the effects of angular diameter and axial ratio (both of which are incorporated in the weight) on the apparent frequency of rings, and to find out whether the trends are sensitive to family. Once again, spiral and lenticular galaxies are treated separately.

The relative frequencies appear to be particularly sensitive to $\log R_{25}$. This is illustrated in Figure 7. Among the spirals having angular diameters $D_0 > 2'.0$ (Fig. 7*a*) the relative frequencies of both the (*r*) and

© American Astronomical Society • Provided by the NASA Astrophysics Data System

1980ApJS...44..451D

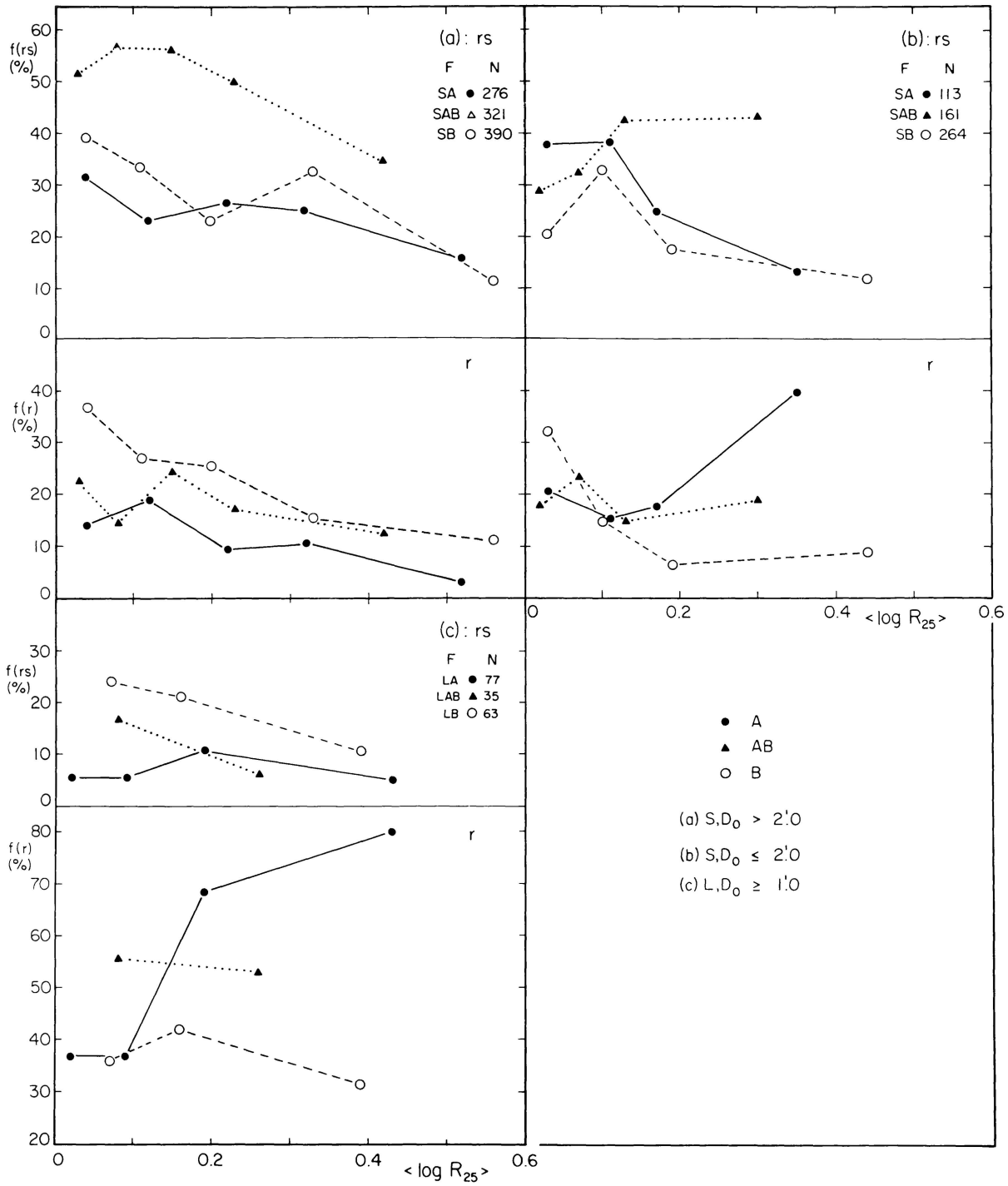

FIG. 7.—Relative frequencies of the (r) and (rs) varieties plotted as functions of log R_{25}. The statistics are separated by family and variety with the total number of objects at each family given in the upper right corner of each separate box. The individual mean points are for bins of log R_{25} including approximately equal numbers of objects determined by the total number N in each family. Spiral and lenticular galaxies are separated, and the statistics in each case are limited to galaxies satisfying the diameter restrictions indicated in the lower right box of the figure.

© American Astronomical Society • Provided by the NASA Astrophysics Data System

1980ApJS...44..451D

(*rs*) varieties decrease substantially with increasing $\log R_{25}$. For example, the relative frequency of the (*r*) variety ranges from $f(r) = 14.0$, 22.4, and 36.7% for SA, SAB, SB galaxies, respectively, at $\langle \log R_{25} \rangle = 0.03$–0.04, to $f(r) = 3.4$, 12.5, and 11.5% at $\langle \log R_{25} \rangle = 0.42$–0.56. For the (*rs*) variety, the values of the relative frequency vary from $f(rs) = 31.6$, 51.7, and 39.2% at $\langle \log R_{25} \rangle = 0.03$–0.04 to $f(rs) = 15.5$, 34.4, and 11.5% at $\langle \log R_{25} \rangle = 0.42$–0.56. These statistics show conclusively that rings are more difficult to detect in spirals of high inclination. However, Figure 7*b* shows that the trend is not so clear among objects having $D_0 < 2'.0$, particularly for the SA(*r*) galaxies. There appears to be an excess of strongly inclined SA(*r*) objects among the smaller galaxies. Such a trend could be an artifact caused by failure to recognize bars in small, highly-tilted objects, or by a misinterpretation of the spiral pattern.

Among the lenticular galaxies, the relative frequency of the (*r*) variety shows a strong dependence on $\log R_{25}$ only for the LA galaxies, as shown in Figure 7*c*. The relative frequencies here were calculated in the same manner as for the spirals, but because of the much smaller sample size the restriction in D_0 was relaxed to include only objects having $D_0 \geq 1'.0$. Whereas the relative frequencies of the LB(*r*) and LAB(*r*) objects show only a small decline with increasing $\log R_{25}$, the LA(*r*) galaxies show a reversed trend from $f(r) = 36.8\%$ at $\langle \log R_{25} \rangle = 0.02$ to $f(r) = 80\%$ at $\langle \log R_{25} \rangle = 0.43$. The excess of the ring variety among the nonbarred lenticulars, noted earlier (§ II*b*), is probably an artifact due to the difficulty of classification of inclined objects. In moderately inclined lenticular galaxies the ring variety is sometimes distinguished by the presence of a narrow arc of dust inside the lens. An example is NGC 4459 shown in the *Hubble Atlas* (Sandage 1961). In edge-on lenticular galaxies, however, the ring appears too foreshortened to be easily distinguished, but its presence is sometimes *inferred* from the existence of a short, narrow absorption band with bright ansae centered about the nuclear region and along the length of the lens. An example is NGC 4710, also shown in the *Hubble Atlas*. It therefore may be that many of the strongly inclined lenticular galaxies classified as LA(*r*) are not of the (*r*) variety at all. Also, the difficulty of classification of family may play a role here, since barred lenticular galaxies are likely to be difficult or impossible to distinguish among edge-on objects.

We conclude from Figure 7 that restriction of the statistics to $\log R_{25} \leq 0.15$–0.20 yields more representative values of the true frequencies of the (*r*) and (*rs*) varieties among the spirals. Among the lenticular galaxies the evidence is not so clear, but a similar restriction should apply.

The dependence on weight of the relative frequencies of varieties among the spirals is shown in Figure 8*a*. The dependence on weight for the (*r*) variety is only slight; for example, among the SB spirals $f(r)$ increases from 18% at $\langle W_T \rangle = 1.8$ to 24% at $\langle W_T \rangle = 4.1$. An opposite trend occurs for the SA(*r*) spirals; here $f(r)$ *decreases* from 22% at $\langle W_T \rangle = 2.0$ to 11% at $\langle W_T \rangle = 4.5$, and an almost identical trend occurs among the SA(*rs*) spirals. This peculiar result may be explained by the fact that most of the low weight classifications in the RC2 are based on the Palomar Sky Survey prints, where overexposure and poor resolution are likely to cause spiral arms to mimic ring structures, and varieties

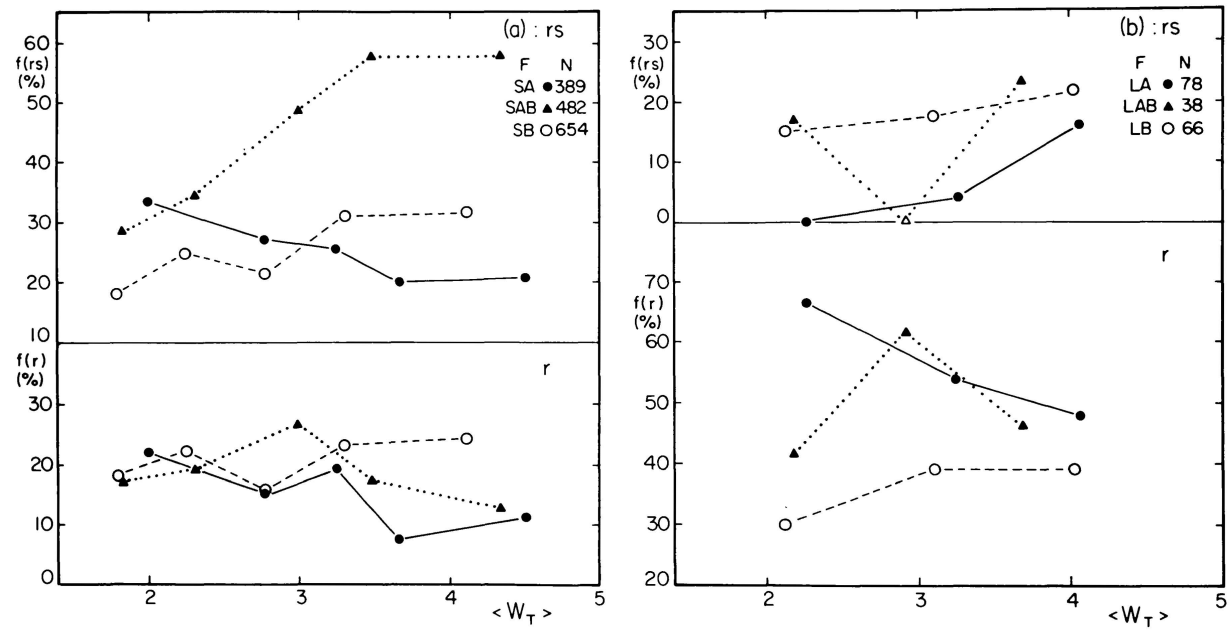

FIG. 8.—Relative frequencies of the (*r*) and (*rs*) varieties as functions of RC2 weight, (*a*) for spirals and (*b*) for lenticulars. The statistics in each case are separated by family and variety; *N* is the total number of objects in each family. The relative frequencies were determined in the same manner as for Fig. 5.

© American Astronomical Society • Provided by the NASA Astrophysics Data System

1980ApJS...44..451D

are either not given or uncertain.

One other interesting trend shown in Figure 8*a* is the substantial increase in the relative frequency of the SAB(*rs*) types with increasing weight. Here $f(rs)$ increases from 28% at $\langle W_T \rangle = 1.8$ to 58% at $\langle W_T \rangle = 4.3$. These results show once again that recognition of the (*rs*) variety requires high resolution and is most frequent among the weakly barred galaxies.

The dependence of the relative frequencies on weight for the lenticulars is shown in Figure 8*b*. For the LB(*r*) and LB(*rs*) galaxies there is a slight increase in the relative frequencies with weight, but the reverse occurs for the LA(*r*) galaxies. There is an excess of LA(*r*) galaxies among the low weight lenticulars. For the LAB galaxies, it is difficult to assign any significance to the trends because of the small sample size.

The dependence of the relative frequencies on $\log D_0$ for the spirals is shown in Figures 9*a* and 9*b*. Here the statistics have once again been separated according to $\log R_{25}$. Figure 9*a* shows that for the SB(*r*) galaxies of low inclination ($\log R_{25} \leq 0.2$) $f(r)$ increases smoothly from 13% at $\langle \log D_0 \rangle = 1.06$ to 31% at $\langle \log D_0 \rangle = 1.64$, where it appears to level off. The trend is weaker among the SAB(*r*) galaxies, but once again $f(r)$ decreases among the SA(*r*) galaxies, varying from about 20% at $\langle \log D_0 \rangle = 1.2$ to 11% at $\langle \log D_0 \rangle = 1.72$. This shows that there is a slight excess of the (*r*) variety among the smaller SA spirals. The effect is more pro-

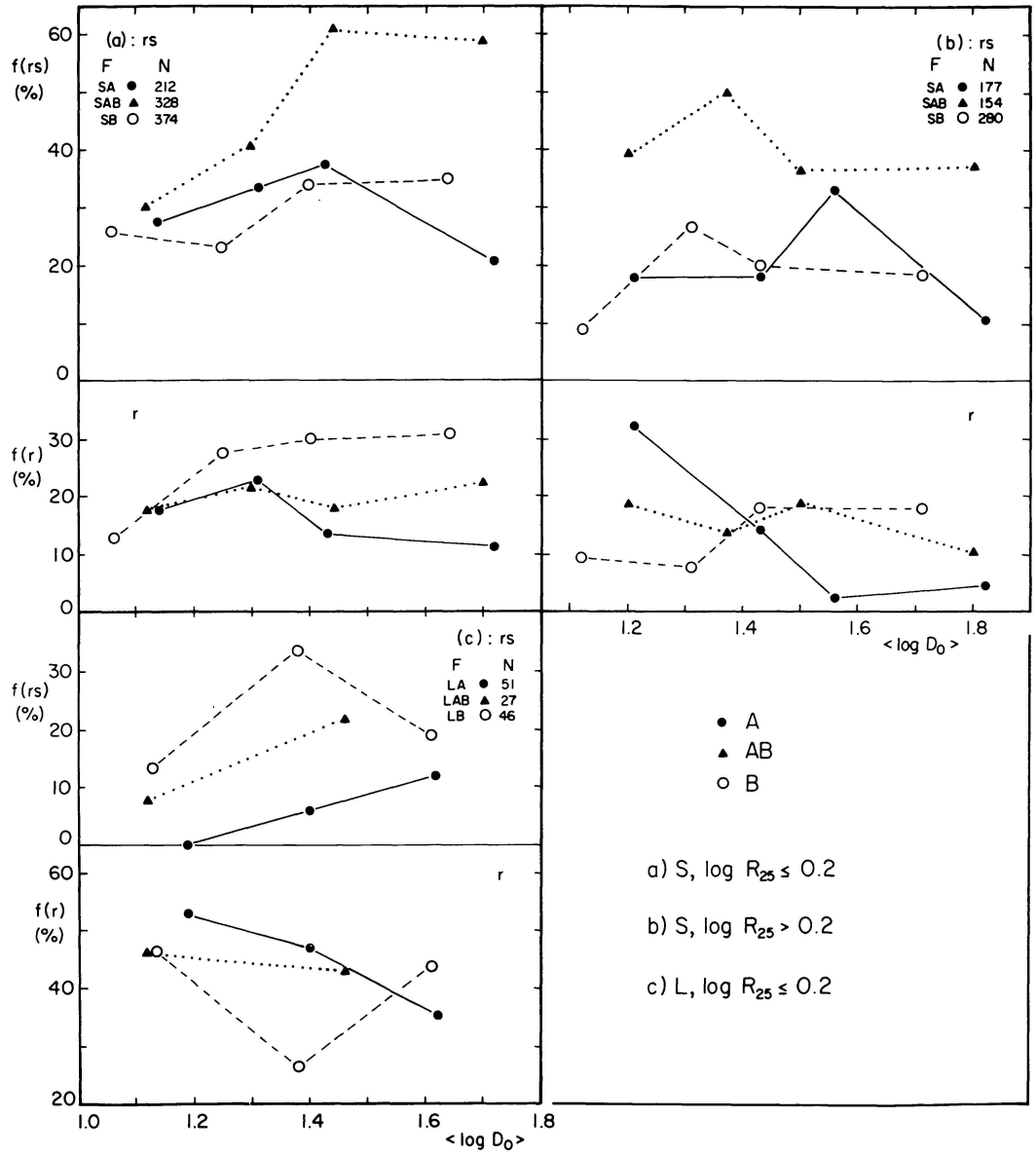

FIG. 9.—Relative frequencies of the (*r*) and (*rs*) varieties as functions of $\log D_0$. The format of the figure and the method used to determine the relative frequencies are identical to those used for Fig. 5. Restrictions according to axis ratio for each class of galaxies are given in the lower right box of the figure.

© American Astronomical Society • Provided by the NASA Astrophysics Data System

1980ApJS...44..451D

nounced for $\log R_{25} > 0.2$, as shown in Figure 9*b*, where $f(r)$ varies from 32% at $\langle \log D_0 \rangle = 1.21$ to less than 5% at $\langle \log D_0 \rangle > 1.5$. This illustrates once again how the statistics of small galaxies of high inclination or low weight may be severely affected by systematic errors of classification.

The analogous statistics with respect to $\log D_0$ for the lenticulars are shown in Figure 9*c* ($\log R_{25} \leq 0.2$ only). The samples here are very small, however, (~20 or less per interval), so that the statistics are not very significant. Nevertheless there appears to be an excess of LA(r) galaxies among the small lenticulars of low inclination.

III. COMPARISON OF RING DIAMETERS AND AXIS RATIOS

a) Comparison of Independent Measurements of Ring Diameters

As noted in § I, the senior author measured major and minor axis diameters of rings in over 400 spiral and lenticular galaxies on large-scale reflector plates during the reclassification of the brighter galaxies on the revised Hubble system; the diameters are given the in notes to RC1. Kormendy (1979) has remeasured the major and minor axis diameters of rings in 43 LB and SB galaxies on the POSS plates, the *Hubble Atlas* and, in a few cases, on new large-scale plate material. All 43 of Kormendy's objects are included among the RC1 measurements. A comparison of the independent measurements will allow us to estimate the measuring errors of ring diameters and axis ratios.

Figure 10*a* shows the correlation between Kormendy's ring diameter measurements D_2 and the corresponding RC1 measurements D_1. Only one point, NGC 1353, is highly discrepant; whereas the RC1 gives a value of 1.'05 for the diameter of the pseudoring in NGC 1353, Kormendy measured 2.'58. We believe that Kormendy did not measure the inner ring of the galaxy, but rather the outer spiral arms which may give the impression of a weak ring. Assuming equal weights for the two sets, the 42 remaining objects give the impartial line

$$D_2 - 1.38 = \underset{\pm 0.034}{0.979}\ (D_1 - 1.36), \qquad (1)$$

with a standard deviation $\sigma = 0.'12$ or, after 2σ rejection of N1784 and 4448,

$$D_2 - 1.39 = \underset{\pm 0.029}{0.977}\ (D_1 - 1.37), \qquad (2)$$

with $\sigma = 0.'10$. The slopes are not significantly different from unity. If the internal errors are assumed to be the same for the two sets of measurements, the standard deviation $\sigma_{12} = 0.'10$ implies individual mean errors $\sigma_1 = \sigma_2 = 0.'07 = 4''$ or relative errors $\sigma/\langle D \rangle = 0.07/1.38 = 5\%$. This confirms that ring diameters are easy to measure unambiguously and with much better internal and external consistency than isophotal diameters of galaxies where errors of 20% are common.

The correlation between the Kormendy and RC1 measurements of ring axis ratios is illustrated in Figure 10*b*. As might be expected, there is more scatter in this correlation than in the diameter correlation, and at least three points, NGC 1784, 2835, and 7723, compare very poorly. The least squares solution after rejection of these points yields for the equal weights impartial line:

$$R_2^{-1} - 0.64 = \underset{\pm 0.052}{1.064}\ (R_1^{-1} - 0.65), \qquad (3)$$

where $R^{-1} = (b/a)$ for the ring. Again, the slope is not significantly different from unity. The standard deviation $\sigma_{12} = 0.06$ gives $\sigma_1 = \sigma_2 = 0.04$ for the individual mean errors of the axis ratios.

These two analyses show that ring diameter measurements are easily duplicated by independent observers provided that reasonably good plate material is used.

b) Comparison of Axis Ratios of Rings and Parent Galaxies

In the RC2 the axis ratio, a/b, of a galaxy at the $\mu_B = 25.0$ mag arcsec^{-2} isophote level is denoted R_{25}.

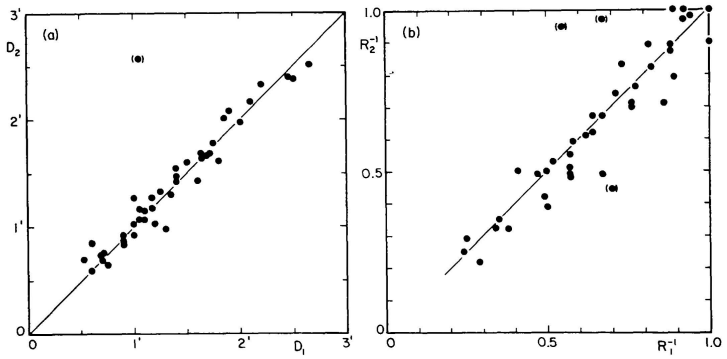

FIG. 10.—Comparison of independent measurements of (*a*) ring major axis and (*b*) ring axis ratio for 43 barred galaxies in common to RC1 and Kormendy (1979). Here D_1 and R_1 refer to the measurements given in the notes to the RC1; D_2, R_2 refer to those by Kormendy. The inverse axis ratio, R^{-1}, is the ratio of the minor to the major axis of the ring. The lines drawn in both (*a*) and (*b*) are of unit slope.

© American Astronomical Society • Provided by the NASA Astrophysics Data System

1980ApJS...44..451D

Let $R_r = (a/b)$ be the corresponding axis ratio for the rings. A comparison between $\log R_r$ and $\log R_{25}$ could shed light on the thickness and true shape of the rings. In this section we compare the axis ratios of the ring and galaxy as a function of family and stage, based on the ring measurements given in RC1. The sample includes both (r) and (rs) galaxies, a combination which we will justify in § IV.

Figures 11–13 show the correlations between $\log R_r$ and $\log R_{25}$ for classes S and L separated by families (A, AB, B) and stages (T). A line of slope +1 is also indicated on each graph. If both ring and galaxy were of the same shape in the plane of the galaxy, with the same intrinsic thickness, then the points would cluster about the 45° line. However, in all three cases $\log R_r > \log R_{25}$, and the effect becomes especially noticeable at the larger values of $\log R_{25}$. This trend over all three families indicates that rings tend to appear more ellipti-

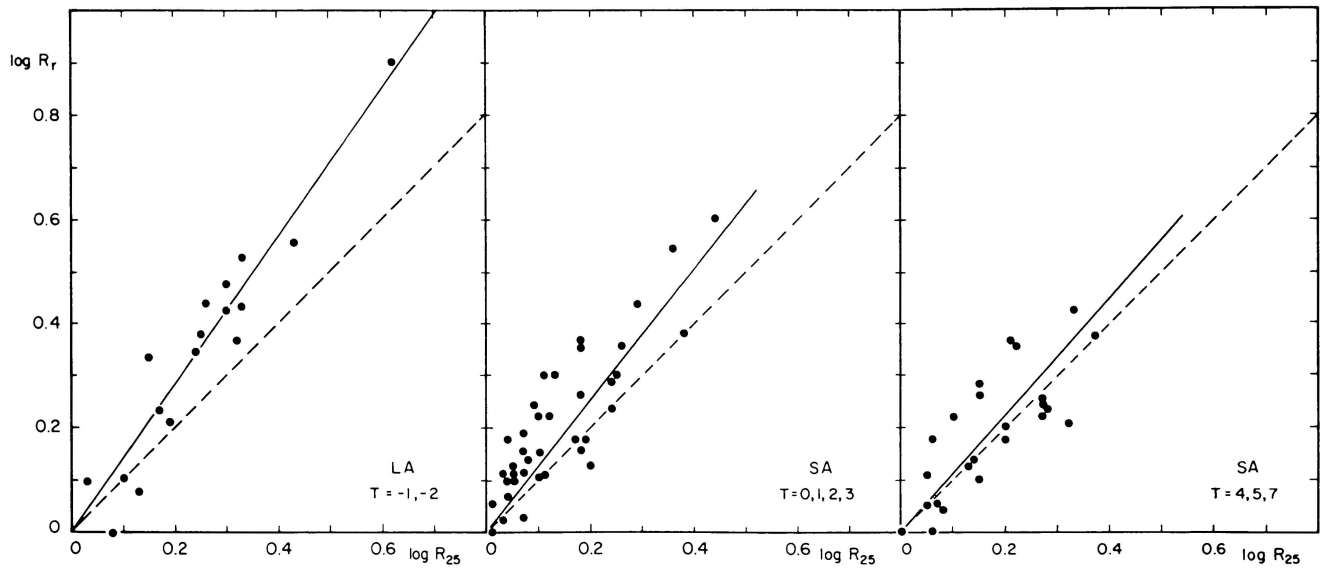

FIG. 11.—Logarithmic plots of ring axis ratios R_r versus RC2 galaxy isophotal axis ratios R_{25} for 80 nonbarred galaxies having ring diameter measurements in RC1. The graphs include both the (r) and (rs) varieties, and the galaxies have been separated according to three intervals of revised Hubble stage: lenticular, early spiral, and late spiral galaxies. The solid line on each graph is based on the least squares coefficients given in Table 5; the slopes were calculated for the types $T = -1$, 2, and 5, which are near the mean types in each interval as given in Table 4. The dashed line on each graph is of unit slope.

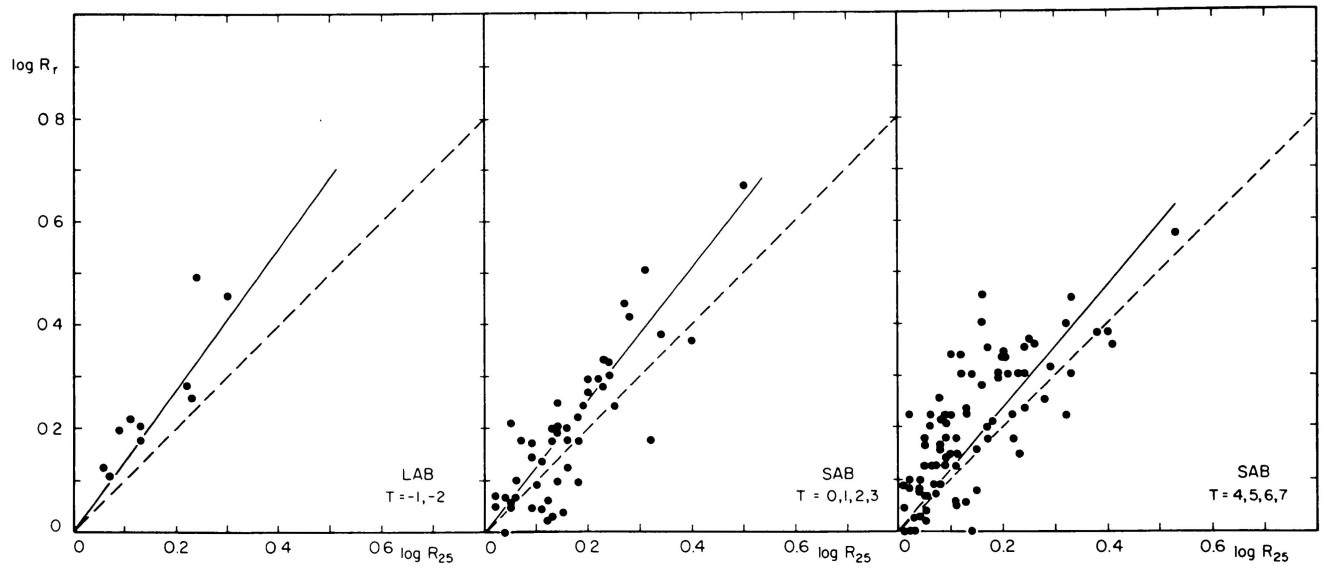

FIG. 12.—Logarithmic plots of R_r versus R_{25} for 151 intermediate barred galaxies having ring diameter measurements in RC1. The format of the graphs is the same as that in Fig. 11. The solid lines are the slopes for $T = -1$, 2, and 5 determined from the least squares solution in Table 5.

© American Astronomical Society • Provided by the NASA Astrophysics Data System

1980ApJS...44..451D

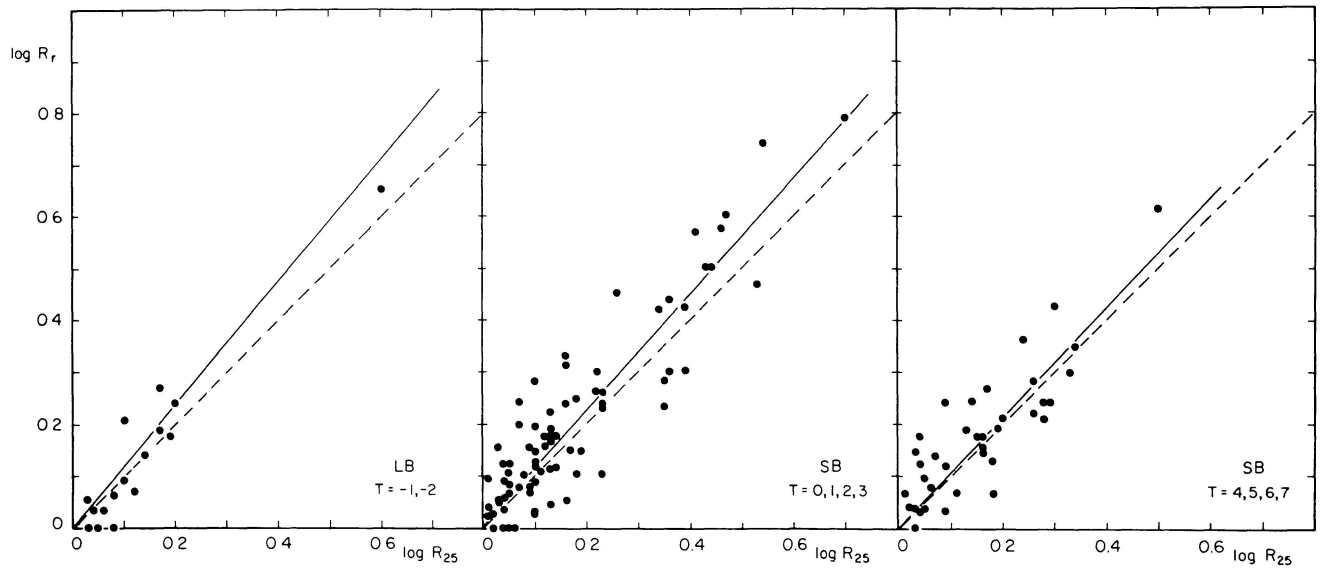

FIG. 13.—Logarithmic plots of R_r versus R_{25} for 131 barred galaxies having ring diameter measurements in RC1. Again, the format of the graphs is the same as that in Fig. 11, and the solid lines are the slopes for $T=-1$, 2, and 5 determined from the least squares solution in Table 5.

cal than the outer parts of the galaxy as outlined by the standard isophote. There is a simple explanation for this effect: rings are flat structures while the isophotal surface corresponding to the standard isophote is influenced by the spheroidal component, especially in highly tilted galaxies. A test of this hypothesis would be to show that the amplitude of the effect depends on stage T, since, as is well known, the strength of the spheroid decreases along the Hubble sequence (de Vaucouleurs 1977, Fig. 17).

The type dependence was studied in two ways. Initially, a two parameter impartial line solution of the form

$$\log R_r = a + b \log R_{25} \qquad (4)$$

was calculated for each of three stage intervals: lenticular ($-2 \leq T \leq -1$), early spiral ($0 \leq T \leq 3$), and late spiral ($4 \leq T \leq 6$) galaxies. The solutions revealed that the slope coefficient b, *decreases* with *increasing* T for each family and that the rate of decrease for a given type depends slightly on family. These solutions are summarized for each family in Table 4, and the slopes are plotted versus $\langle T \rangle$ (the average T in each interval) in Figure 14. It shows that the dependence on type is strongest for the SA galaxies and weakest for the SB galaxies, and that within the rather large mean errors the decrease is roughly linear. Table 4 also shows that, within the errors, the values of the intercepts in the impartial relations are not significant. These results imply that a relation of the form

$$\log R_r = (c + dT) \log R_{25} \qquad (5)$$

represents adequately the variation over the whole range of types T. Values of the coefficients c and d are collected in Table 5 for the three families, and the solutions are illustrated for the three T intervals mentioned above in Figures 11–13.

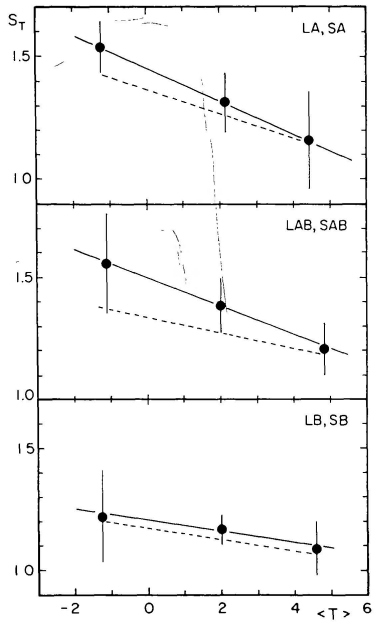

FIG. 14.—Plots of the slope, $S_T = \partial \log R_r / \partial \log R_{25}$, as a function of revised Hubble stage and family. The solid dots with error bars indicate the slopes b given in Table 4, calculated from least squares solutions to equation (4); a solid line has been drawn to connect these points. The dashed lines represent the variation of S_T with T as indicated by the least squares solutions to equation (5). The differences in $\partial S_T / \partial T$ determined from the two methods are due partly to size of sample differences in the three intervals of stage and partly to regression effects.

© American Astronomical Society • Provided by the NASA Astrophysics Data System

1980ApJS...44..451D

TABLE 4

COEFFICIENTS OF EQUATION (4)[a]

Family	⟨T⟩	a (m.e.)	b (m.e.)	N	σ[b]	Rejected	Log R Range
SA.....	−1.24	−0.034 ±0.029	1.537 ±0.108	17	0.06	N4124	0.72
	+2.15	+0.024 ±0.018	1.311 ±0.122	39	0.07	N5472	0.50
	+4.43	−0.007 ±0.034	1.159 ±0.200	23	0.08	N1659, 2535	0.38
SAB	−1.10	+0.006 ±0.033	1.556 ±0.202	10	0.05	N2962	0.29
	+2.02	−0.032 ±0.019	1.383 ±0.111	48	0.07	N779, 1424, 2852, 3166, 5379	0.57
	+4.85	+0.026 ±0.015	1.207 ±0.109	92	0.09	N4899, 5885, 5899, 5967, 7314	0.54
SB.....	−1.24	−0.031 ±0.027	1.219 ±0.19	17	0.05	N2983, 7155	0.61
	+2.00	+0.003 ±0.013	1.167 ±0.06	76	0.08	N5298, 5566, 6754	0.74
	+4.61	+0.013 ±0.019	1.088 ±0.110	36	0.07	N613, 3198, 7393, I5201	0.54

[a]Impartial line solution after 2σ rejection.
[b]Standard deviation from impartial line after 2σ rejection.

TABLE 5

COEFFICIENTS OF EQUATION (5)[a]

Family	c (m.e.)	d (m.e.)	N	σ
a) All Galaxies				
SA.....	1.367 ±0.047	−0.050 ±0.018	80	0.076
SAB	1.338 ±0.074	−0.032 ±0.019	151	0.084
SB.....	1.165 ±0.049	−0.022 ±0.017	131	0.070
b) $D_o > 2'.0$ only				
SA.....	1.349 ±0.049	−0.057 ±0.018	57	0.072
SAB	1.397 ±0.079	−0.041 ±0.020	129	0.083
SB.....	1.185 ±0.044	−0.022 ±0.017	111	0.068

[a]After rejection of galaxies listed in Table 4.

The solutions in Tables 4 and 5 show the variation with type that would be expected if the trend $\log R_r > \log R_{25}$ is due mainly to a combination of the effect of the bulge-to-disk ratio on the minor axis measurement of a flat galaxy and the fact that rings are themselves flat. In particular, the slope $b(T) = \partial \log R_r / \partial \log R_{25}$ approaches unity for the later-type galaxies where the bulge is minimal, but it is significantly greater than unity for the early-type galaxies where the bulge is dominant. The dependence of the slope on family is perhaps harder to explain; however, such a dependence could arise if the thickness of the *spheroid* in barred galaxies is *smaller* than that in nonbarred galaxies.

Finally, it should be noted that the form of equation (5) adopted to express the correlation between these two variables is only a first order representation. We have neglected a possible second order effect related to the intrinsic shapes of inner rings (circular versus elliptical) in their own plane, an effect which may be present among the barred spirals (de Vaucouleurs 1970), although this has been disputed (Kormendy 1979). A statistical discussion will be presented later by one of us (R. B.), but for the present we can observe that in cases where the plane of vision includes the bar (as in NGC 1326, 1398, 3351, and others) and the ring appears nearly circular, the galactic disk appears always elongated with its major axis at right angles to the bar, an improbable coincidence if it is assumed that the disk is noncircular in its own plane, but a necessary consequence of the geometry if the ring is elliptical with its major axis along the bar (Fig. 15).

IV. DIMENSIONLESS SYSTEMATICS OF INNER RINGS: DEFINITIONS OF THE PARAMETERS X AND Y AND REPRESENTATIONS OF THEIR DEPENDENCE ON FAMILY, STAGE, VARIETY, AND LUMINOSITY CLASS

The study of dimensionless ratios of the apparent diameters of major structural components of galaxies and their dependence on various parameters is useful because it allows one to isolate trends which are intrinsic to the galaxy (i.e., not affected by distance). In the case of inner rings, we have studied the ratios D_o/D_r and A_e/D_r and their dependence on type, family, variety, and luminosity class. Here D_o is the corrected

© American Astronomical Society • Provided by the NASA Astrophysics Data System

1980ApJS...44..451D

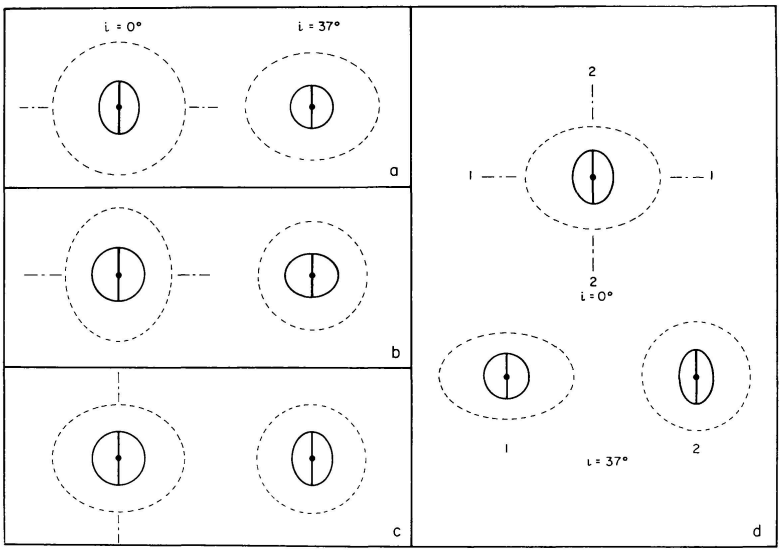

FIG. 15.—Possible combinations of intrinsic shapes of inner ring and outer disk in a barred spiral: (*a*) axisymmetric disk with an elliptical ring having $b/a=0.8$. When the galaxy is tilted 37° about an axis perpendicular to the bar in the plane of the sky, the ring will appear to be circular, while the disk has an apparent axial ratio of 0.8. An example of a galaxy with this aspect is NGC 3351 (Fig. 3*e*); (*b*) circular ring with elliptical disk having its major axis parallel to the bar and $b/a=0.8$. By tilting the galaxy 37° about the same axis as in (*a*), the outer disk appears circular while the ring appears elliptical with major axis *perpendicular* to the bar. Such a configuration has not been observed; (*c*) circular ring with elliptical disk having its major axis perpendicular to the bar and axis ratio 0.8. Tilting the galaxy about the axis shown makes the disk look circular and the ring elliptical with major axis along the bar; (*d*) a special case where both the inner ring and outer disk are elongated with axis ratios of 0.8 but with major axes perpendicular to each other. Tilting the galaxy 37° about axis 1 makes the inner ring circular and the disk highly elliptical with an axis ratio of 0.64. Tilting the galaxy about axis 2 makes the disk circular but the ring appears highly elliptical with an axis ratio 0.64. An example of a galaxy resembling this case is NGC 1326 (Fig. 3*b*).

face-on isophotal diameter of a galaxy as defined in the RC2, and A_e is the effective aperture which transmits half the total flux of a galaxy. By its definition, A_e is a metric diameter. Hence, A_e/D_r is the dimensionless ratio of two metric lengths and is in a sense a more intrinsic quantity than D_0/D_r, which depends on surface brightness. However, only 40% of the galaxies in our sample have A_e values in the RC2, while all have a D_0, so it is worthwhile to consider both types of diameters. We show in this section that both ratios depend on family and stage, and that the dependence on family (i.e., A versus B) allows us to quantify the concept of bar strength as a continuous parameter from SA to SB. In fact, we have found that the refined family classification symbolism (AB and $\overline{\text{AB}}$) used by de Vaucouleurs (1963*a*) is especially significant in this connection, and we have utilized these refinements in our analyses. We also show that the (*r*) and (*rs*) varieties have similar properties and can be treated together rather than separately, and that the ratios have no significant dependence on luminosity class.

a) *Dependence on Variety*

Using the large sample of galaxies with ring measurements from the RC1, we have calculated values of the parameter $X=\log D_0/D_r$ for 423 objects and of the parameter $Y=\log A_e/D_r$ for 166 objects (D_0 and A_e are taken from RC2). To test for a possible dependence of these parameters on variety, we compare in Table 6 the mean values of X and Y between the pure ring (*r*) and pseudoring (*rs*) varieties, separating the statistics by family (A, AB, B) and class (L, S). A dependence of these parameters on variety might be expected since pseudo inner rings tend to appear more open or incomplete than pure inner rings, especially if the (*s*) characteristic dominates. Table 6 shows, however, that in general $\langle X\rangle$ and $\langle Y\rangle$ are the same for the (*r*) and (*rs*) types within the mean errors and that this is true for both classes of galaxies and for each family. The same type of behavior carries into the dependence of X and Y on stage (see § IV*b*): (*r*) and (*rs*) galaxies are found not to be strongly segregated from one another, although the (*rs*) variety does carry into later stages than the (*r*) variety. We have also checked that exclusion of about 40 *s*-dominated pseudorings (galaxies classified by de Vaucouleurs [1963*a*] as [$\overline{rs}$]) in our sample does not change the averages in Table 6 significantly. These results indicate that the relative scale of the two varieties is nearly the same (in Paper II we will show that this is also true for the linear diameter of the rings), and hence that they can be treated together. We do this in all of our succeeding analyses with X and Y.[4]

[4]From a more detailed analysis it is found that X and Y may have a very slight dependence on variety. If one uses the least squares solutions derived in § IV*b*(i) to correct X and Y for their type and family dependences, a slight dependence on variety is found such that X and Y decrease from (*r*) to (*rs*) by perhaps 0.03–0.04. However, the variation is barely significant and much smaller than the dominant effects of T and F; it will be neglected in what follows, particularly since the finer classification is not available for the majority of galaxies.

© American Astronomical Society • Provided by the NASA Astrophysics Data System

1980ApJS...44..451D

TABLE 6

COMPARISON OF STATISTICS FOR (*r*) AND (*rs*) GALAXIES[a]

Family and Variety	$\langle X\rangle_S$ (m.e.)	N	$\langle X\rangle_L$ (m.e.)	N	$\langle Y\rangle_S$ (m.e.)	N	$\langle Y\rangle_L$ (m.e.)	N	$\langle D_l\rangle_S$ (m.e.)	N
A(*r*)	0.78	33	0.51	24	0.32	13	−0.06	9	3.1	9
	±0.04		±0.05		±0.07		±0.095		±0.4	
A(*rs*)	0.72	33	(0.67)	1	0.27	14	(0.09)	1	3.7	15
	±0.03		...		±0.04		...		±0.4	
AB(*r*)	0.64	53	0.38	9	0.23	18	(−0.25)	1	4.6	26
	±0.03		±0.03		±0.05		...		±0.6	
AB(*rs*)	0.69	115	0.48	2	0.24	50	−0.11	2	4.1	71
	±0.01		±0.10		±0.03		±0.23		±0.3	
B(*r*)	0.50	69	0.43	15	0.05	25	−0.11	5	7.9	30
	±0.015		±0.03		±0.03		±0.085		±0.6	
B(*rs*)	0.50	61	0.48	8	0.00	24	0.00	4	6.6	29
	±0.02		±0.06		±0.035		±0.05		±0.6	

[a] $X=\log D_0/D_r$, $Y=\log A_e/D_r$; L=lenticulars; S=spirals; D_l=linear diameter of ring in kpc based on μ_0^v distance moduli (de Vaucouleurs 1979*b*).

b) *Dependence on Family and Stage*

i) *Least Squares Solutions*

Figures 16 and 17 show the dependence of X and Y on stage T, separated by family. Some general features of these graphs to be noted are as follows: (1) both X and Y are smallest among the lenticular galaxies and each shows a tendency to increase in the later stages among the spirals; (2) both parameters decrease from SA to SB spirals, while among lenticulars they remain roughly constant for all three families (see Fig. 18); (3) Y appears to increase more rapidly toward later types T than does X; and (4) the scatter of the data points is smallest for the SB galaxies and largest for the SA galaxies.

In an attempt to represent both the type and family dependence of X and Y, solutions of the form

$$X, Y = a_0 + a_1 F + (b_0 + b_1 F) T, \qquad (6)$$

were experimented with over the spiral sequence only. Here F denotes a numerical *family index*, arbitrarily chosen to be −1 for SA, −0.5 for SAB, 0.0 for SAB, +0.5 for SAB, and +1 for SB galaxies. The necessity for considering family in this manner is illustrated

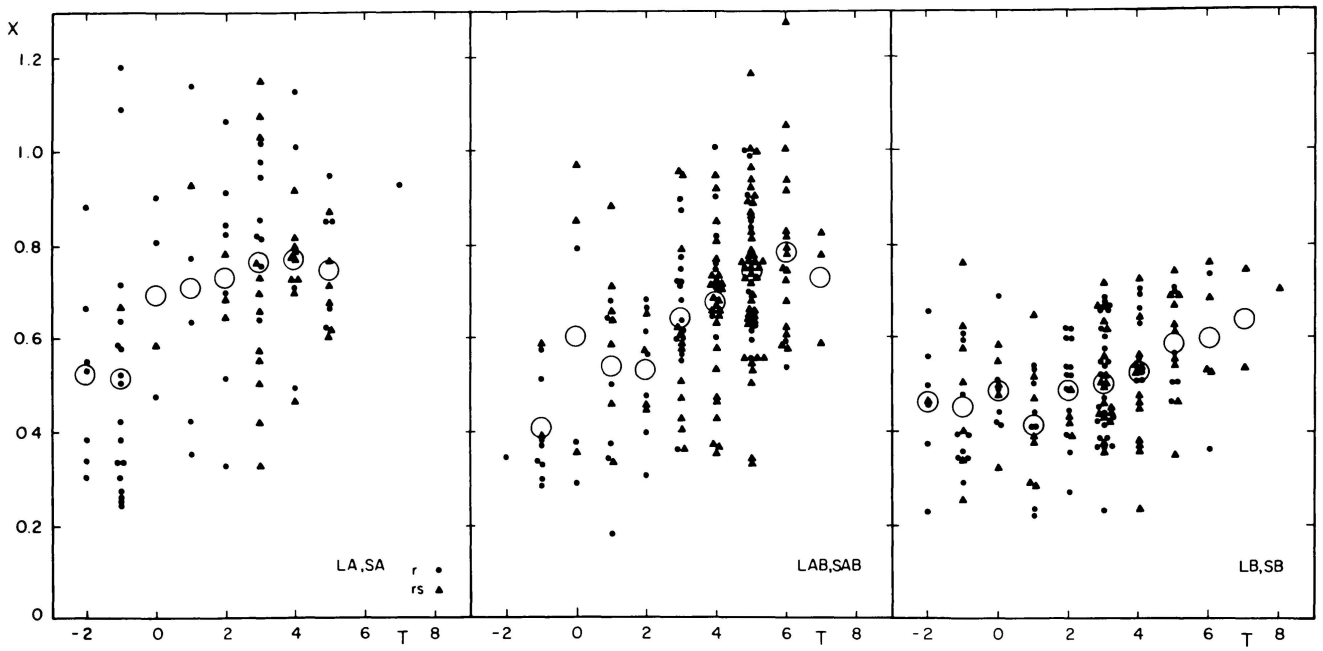

FIG. 16.—Logarithmic diameter ratio $X=\log D_0/D_r$ as a function of stage for 423 spiral and lenticular galaxies. The galaxies are separated by family, and different symbols are used for the (*r*) and (*rs*) varieties. The large open circles indicate the mean values at each stage.

© American Astronomical Society • Provided by the NASA Astrophysics Data System

1980ApJS...44..451D

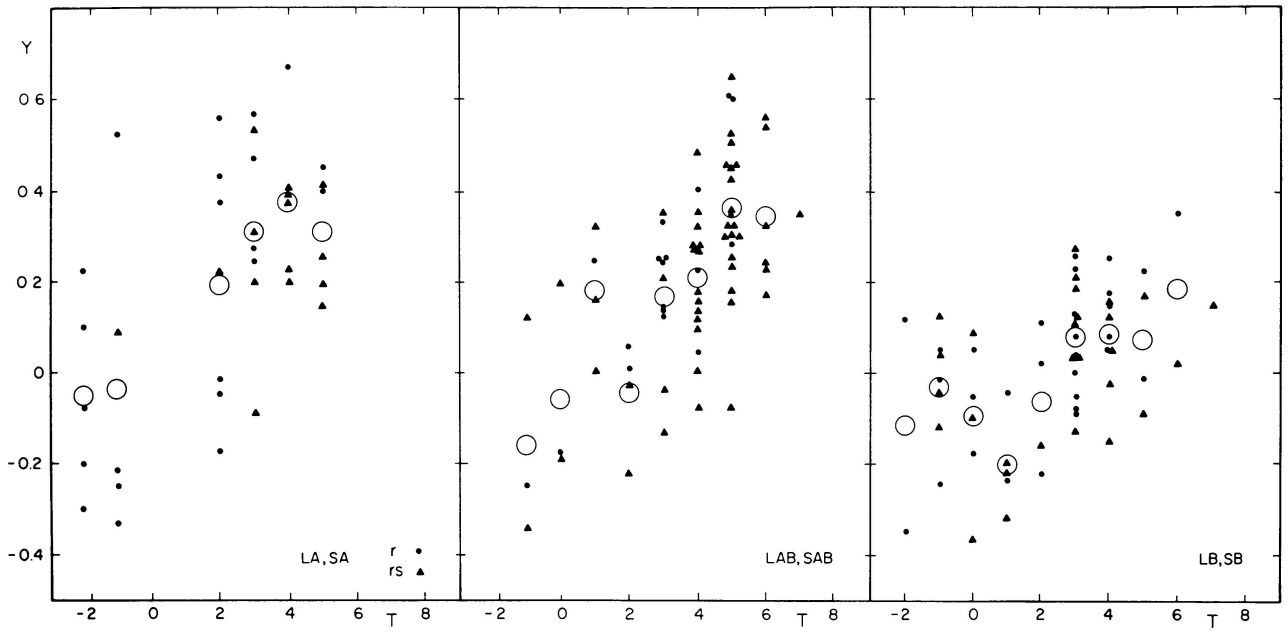

FIG. 17.—Logarithmic diameter ratio $Y = \log A_e/D_r$ as a function of stage for 166 spiral and lenticular galaxies. The format is the same as in Fig. 16.

quantitatively in Figure 18; as will be shown later in this section, these refinements are fairly significant. The solutions were initially restricted only to the spirals because, as was noted in (2), the lenticular galaxies do not appear to show a significant trend with family. The form of the solution above accounts not only for the family dependence of the zero point of each relation, but also for a possible family dependence of the slope. It was found in the initial trials, however, that there is no significant dependence of the slope on family, so that we have set $b_1 = 0$.

Table 7A summarizes the values of the coefficients a_0, a_1, and b_0 for both the (X, F, T) and (Y, F, T) correlations. Only the solutions after 2σ rejection are given; in general, they are essentially the same as those before rejection (rejected points are discussed in § IV*b*[ii]). The solutions for each family are illustrated in Figure 18. It is seen that the slopes of the two relations are significantly different: while the slope $\partial X/\partial T = 0.034 \pm 0.004$ corresponds to an 8% increase in D_0/D_r per unit stage interval, $\partial Y/\partial T = 0.063 \pm 0.008$ corresponds to a 16% increase in A_e/D_r per unit stage interval. On the other hand, Table 7A shows that the coefficient a_1 is the *same* for both correlations. That is, within the mean errors,

$$\frac{\partial X}{\partial F} = \frac{\partial Y}{\partial F} = -0.13$$

which corresponds to a 26% decrease in D_0/D_r and A_e/D_r per unit family interval. The small mean error in each case, (0.01 for $\partial X/\partial F$, 0.02 for $\partial Y/\partial F$) indicates that this coefficient is highly significant. This confirms the conclusion (de Vaucouleurs 1970) that inner rings are smaller (relative to the disk diameter) in ordinary SA spirals than in barred SB spirals as shown in Figure 4.

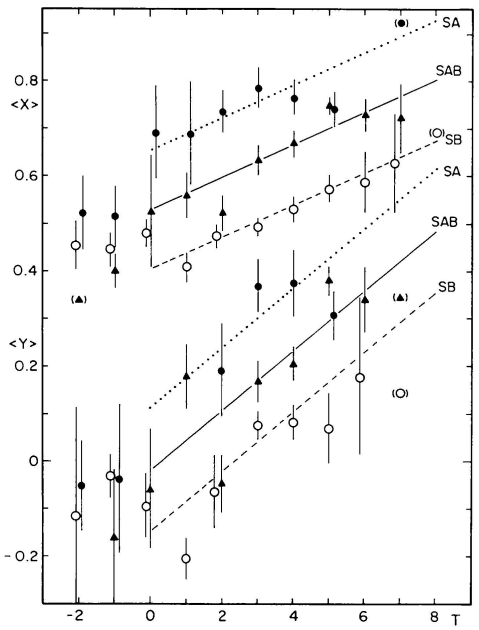

FIG. 18.—Mean logarithmic diameter ratios $\langle X \rangle$ and $\langle Y \rangle$ versus stage T and family. The error bars show the mean errors of the mean points at each stage, and different symbols are used for each family. The straight lines are best fits over the restricted spiral sequence $0 \leq T \leq 8$ from least squares solutions to equation (6) as given in Table 7, sample (*a*). Points rejected from these solutions were also rejected in the calculation of the mean points.

© American Astronomical Society • Provided by the NASA Astrophysics Data System

1980ApJS...44..451D

TABLE 7

COEFFICIENTS OF EQUATION (6)

PARAMETERS	COEFFICIENTS a_0 (m.e.)	a_1 (m.e.)	b_0 (m.e.)	N	σ
		Sample (a)			
X	+0.532 ±0.017	−0.127 ±0.010	+0.034 ±0.004	346	0.14
Y	−0.017 ±0.032	−0.130 ±0.018	+0.063 ±0.008	138	0.15
		Sample (b)			
X	+0.526 ±0.017	−0.126 ±0.010	+0.038 ±0.005	304	0.13
Y	+0.014 ±0.034	−0.137 ±0.019	+0.057 ±0.009	122	0.15
		Sample (c)			
X	+0.566 ±0.023	−0.148 ±0.014	+0.035 ±0.006	184	0.14
Y	+0.023 ±0.039	−0.119 ±0.023	+0.057 ±0.010	85	0.15

NOTES—Sample (a): All spirals, after 2σ rejection of NGC 245, 470, 1068, 2701, 3166, 3182, 3241, 3642, 4389, 4622, 4689, 5660, 5669, 5728, 7059, 7217, and IC 239 from the X solution and NGC 470, 2701, 3241, 5248, and 7217 from the Y solution. Sample (b): Excluding (rs) types, and after 2σ rejection of NGC 245, 470, 1068, 1317, 2701, 3166, 3182, 3241, 3642, 4622, 4689, 5172, 5669, 5728, 7059, and 7217 from the X solution and NGC 470, 2701, 3241, and 4151 from the Y solution. Sample (c): Excluding (rs) types, galaxies having $D_0 \leq 2.0$, $\log R_{25} > 0.2$, and after 2σ rejection of NGC 470, 1068, 2701, 3182, 4622, and 4689 from the X solution and NGC 470, 2701, and 4151 from the Y solution.

As a check on the solutions in Table 7A, we also calculated values of the coefficients a_0, a_1, and b_0 for two restricted subsamples of our main data set: (a) a sample which excludes (s) dominated pseudorings (rs), of which there are about 40 in the main data set, and (b) a similar subsample which also excludes galaxies having $D_0 < 2.0$ and $\log R_{25} > 0.2$. The coefficients in these cases are tabulated in Tables 7B and 7C. It is seen that the slopes b_0 in both cases are virtually identical to those in Table 7A, and that, within the mean errors, $a_1(X)$ and $a_1(Y)$ agree and have the same mean value as in Table 7A. Thus we find that the constants of the correlation are not seriously affected by the inclusion of (rs) galaxies, or of the smaller, highly inclined galaxies.

The value $\langle a_1 \rangle = -0.13$ can be used to reduce the SA, SAB, SAB, and SB galaxies to the SAB case ($F=0$). Once such a reduction is performed, the resulting dependence of the reduced values of X and Y on T can be used to derive a more accurate mean value of the slope coefficient b. Solutions for the coefficients a' and b' in the relations X', $Y' = a' + b'T$, where $X' = X + 0.13F$ and $Y' = Y + 0.13F$, (for the same samples as in Table 7) are tabulated in Table 8. It is seen that the slopes and zero points are essentially the same as in the three-parameter solutions. We adopt therefore the following mean relations as the best representations of the dependence of X and Y on type among the spirals:

$$X = \log D_0/D_r = \underset{\pm 0.02}{0.54} - \underset{\pm 0.01}{0.13F} + \underset{\pm 0.005}{0.036T}, \quad (7a)$$

$$Y = \log A_e/D_r = \underset{\pm 0.03}{0.01} - \underset{\pm 0.02}{0.13F} + \underset{\pm 0.009}{0.059T}. \quad (7b)$$

To illustrate the dependence of the reduced parameters on type, we show in Figure 19 plots of $\langle X' \rangle$ and $\langle Y' \rangle$ versus T (after 2σ rejections). On the same graphs we have also plotted the location of the lenticulars, but in this case we have set $X' = X$ and $Y' = Y$ (i.e., no family dependence). Both graphs show that our linear relations are good representations within the mean errors, including the lenticular galaxies. Hence, the variations of X' and Y' across the entire Hubble sequence can be represented by equations (7), if lenticulars are treated as SAB galaxies ($F=0$).

To check what effect inclusion of the lenticular galaxies would have on our solutions, we recalculated the coefficients a' and b' in Table 8, setting $F=0$ for

© American Astronomical Society • Provided by the NASA Astrophysics Data System

1980ApJS...44..451D

TABLE 8

COEFFICIENTS OF EQUATIONS (7a) AND (7b)

PARAMETERS	COEFFICIENTS a' (m.e.)	b' (m.e.)	N	σ
	Sample (a)			
X'.....	+0.533 ±0.017	+0.034 ±0.004	347	0.14
Y'.....	−0.010 ±0.031	+0.062 ±0.008	139	0.15
	Sample (b)			
X'.....	+0.527 ±0.017	+0.038 ±0.0045	303	0.13
Y'.....	+0.011 ±0.033	+0.058 ±0.009	122	0.15
	Sample (c)			
X'.....	+0.556 ±0.022	+0.035 ±0.006	183	0.14
Y'.....	+0.025 ±0.038	+0.056 ±0.010	85	0.15

NOTES—Sample (a): All spirals, after 2σ rejection of NGC 245, 470, 1068, 2701, 3166, 3182, 3241, 3642, 4622, 4689, 5660, 5669, 5728, 7059, 7217, and IC 239 from the X solution and NGC 470, 2701, 3241, and 5248 from the Y solution. Sample (b): Excluding rs types, and after 2σ rejection of NGC 245, 470, 1068, 1317, 2701, 3166, 3182, 3241, 3642, 4389, 4622, 4689, 5172, 5669, 5728, 7217, and 7531 from the X solution and NGC 470, 2701, 3241, and 4151 from the Y solution. Sample (c): Excluding rs types, galaxies having $D_o \leq 2'.0$, $\log R_{25} > 0.2$, and after 2σ rejection of NGC 470, 1068, 2701, 3182, 4622, 4689, and 7217 from the X solution and NGC 470, 2701, and 4151 from the Y solution.

lenticulars. The results for the same three cases as in Tables 7 and 8 are collected in Table 9, which shows that the coefficients are virtually identical, within the mean errors, to those in Table 8; this confirms that a single linear relation common to the L and S classes is consistent with the data. The following mean relations are the best representations of X' and Y' on type across the entire L–S sequence for $-2 \leq T \leq 8$:

$$X' = \underset{\pm 0.01}{0.52} + \underset{\pm 0.003}{0.041}T\,, \qquad (8a)$$

$$Y' = \underset{\pm 0.02}{0.01} + \underset{\pm 0.006}{0.058}T\,. \qquad (8b)$$

It is interesting to note that equations (7a) and (7b) indicate that the parameter $\log D_o/A_e \equiv X - Y$ should have a slight dependence on type but no dependence on family. To check whether this is the case, values of $\langle \log D_o/A_e \rangle$ versus T were calculated for 175 SA, LA galaxies, 139 SAB, LAB galaxies, and 170 SB, LB galaxies from the RC2, without regard to variety. Figure 20 shows the results. We see that over the range of types under consideration, there is a general, nearly linear decrease of $\log D_o/A_e$ with increasing type T, but that there is no significant dependence on family at

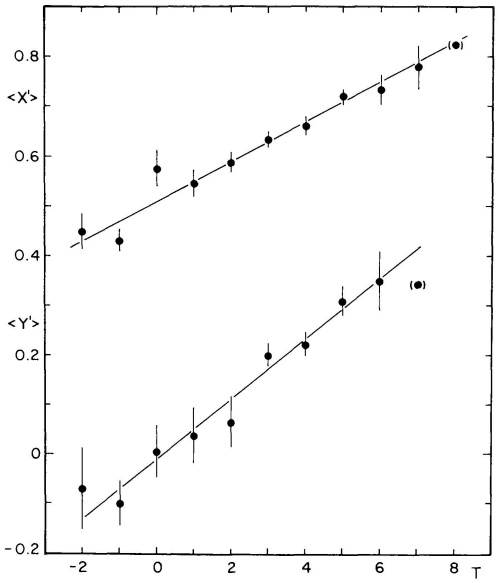

FIG. 19.—Mean values of the reduced parameters $X' = X + 0.13F$ and $Y' = Y + 0.13F$, where F is the family index, as a function of stage T. The straight lines represent the best linear fits over the entire stage sequence according to the least squares solutions given in Table 9, sample (a). Points rejected from these solutions were also rejected in the calculation of the mean points.

TABLE 9

COEFFICIENTS OF EQUATIONS (8a) AND (8b)

PARAMETERS	COEFFICIENTS a' (m.e.)	b' (m.e.)	N	σ
	Sample (a)			
X'.....	+0.509 ±0.011	+0.040 ±0.003	405	0.14
Y'.....	−0.007 ±0.020	+0.061 ±0.006	160	0.16
	Sample (b)			
X'.....	+0.508 ±0.011	+0.042 ±0.003	364	0.14
Y'.....	−0.002 ±0.021	+0.060 ±0.006	144	0.16
	Sample (c)			
X'.....	+0.540 ±0.016	+0.040 ±0.004	208	0.14
Y'.....	+0.034 ±0.024	+0.054 ±0.007	99	0.15

NOTES—Sample (a): All spiral and lenticular galaxies, after 2σ rejection of NGC 245, 470, 1068, 2701, 3166, 3182, 3241, 4124, 4459, 4622, 4689, 5660, 5728, 7059, 7217, 7252, and IC 239 from the X solution and NGC 470, 2701, 3241, 4459, and 5248 from the Y solution. Sample (b): Excluding (rs) types, and after 2σ rejection of NGC 245, 470, 1068, 2701, 3166, 3182, 3241, 3642, 4124, 4459, 4622, 4689, 5728, 7217, and 7252 from the X solution and NGC 470, 2701, 3241, and 4459 from the Y solution. Sample (c): Excluding (rs) types, galaxies having $D_o \leq 2'.0$, $\log R_{25} > 0.2$, and after 2σ rejection of NGC 470, 1068, 2701, 3182, 4459, 4622, 4689, and 7252 from the X solution and NGC 470, 2701, 4151, and 4459 from the Y solution.

© American Astronomical Society • Provided by the NASA Astrophysics Data System

1980ApJS...44..451D

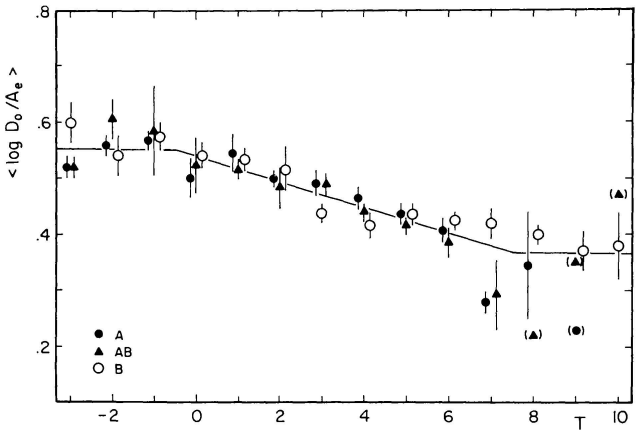

FIG. 20.—Mean logarithmic diameter ratio $\langle \log D_0/A_e \rangle$ vs. stage T for 175 LA, SA galaxies, 139 LAB, SAB galaxies, and 170 LB, SB galaxies taken from the RC2. A number of highly discrepant points were rejected from the means in some cases. The straight line over the range $0 \leq T \leq 8$ is from a least squares solution to the individual points ($\log D_0/A_e = 0.539 - 0.023T$); its coefficients are essentially the same as those in equation (9) which were predicted from equations (7a) and (7b). The horizontal lines for $-3 \leq T \leq -1$ and $T \geq 8$ are means of all the individual points over those ranges.

any stage. In fact, the predicted dependence from equations (7a) and (7b) of $\log D_0/A_e$ on type,

$$X - Y = 0.53 - 0.023T, \qquad (9)$$

adequately represents the variation over the spiral range $0 \leq T \leq 8$. This dependence of $\log D_0/A_e$ on type is an effect of the decreasing central concentration of light in the later spiral stages. Note also that the lack of family dependence in the $\log D_0/A_e$ parameter implies that the rings are solely responsible for such a dependence in the X, Y parameters (this is verified in the Appendix).

ii) *Comments on Rejected Galaxies*

At this point it is worth considering more carefully the galaxies which were 2σ rejected from the X, Y, F, T correlations. There were at least 24 galaxies consistently rejected from these solutions, and the individual rejections for each solution are listed in Tables 7–9. Each of these galaxies was inspected on the POSS plate copies, or on large scale prints or plates where available, to see if a reason for the discrepancy could be found. It is interesting to note that 10 of these 24 objects are SA galaxies, 10 are SAB, but only one is an SB. Of the 10 SAB galaxies rejected, 4 have *s*-dominated pseudorings and were rejected beforehand in some of our solutions (Tables 7A, 7B, 8B, 8C, 9b, and 9C). Some of the rejected SA galaxies are particularly interesting; for example, NGC 4622 appears to be a perfect SA(r) when inspected on a large-scale photograph, yet it has a very large ring compared to the total size of the galaxy, yielding a value of X which is more consistent with the barred spirals. Three other SA galaxies which behave similarly are NGC 245, 470, and 3241. In NGC 245 the low value of X may be due to an incorrect value of D_0; the diameter measurement for this galaxy is based only on an old Heidelberg plate. In NGC 470, the POSS O-plate indicates that a weak bar may be present, while in NGC 3241 the POSS E-plate reveals a definite, straight bar crossing the round nuclear region (but this bar is practically invisible on the corresponding O plate). Even more interesting are a few cases where the inner ring is relatively strong, but very little structure appears to be outside the ring so that X is again very small. Two galaxies in the rejection list, NGC 4389 and 5728, are like this. NGC 4389 resembles the large nearby ringed spiral NGC 4725, but appears virtually only as a ring-plus-bar on the POSS plates. NGC 5728 has a central region which is more like a lens with a weak bar in it, but the rim of the lens resembles a ring structure, or at least a tightly wound spiral pattern around the bar (see Sandage and Brucato 1979). One other galaxy which behaves similarly to these two but which was not 2σ rejected is NGC 1512. This galaxy has one of the most conspicuous of all ring structures, yet outside the ring the spiral structure is so weak that it can be detected only on very deep photographs (see, e.g., Sandage and Brucato 1979).

At the other extreme, there are cases where X is abnormally large compared to the mean at a given stage. Two of the most interesting of these cases are NGC 1068 and 7217. NGC1068 is a bright Seyfert galaxy having a very small, high-surface-brightness, inner pseudoring structure; a weak multiarmed spiral pattern emerges from this ring forming an intermediate region which could be called a lens (Kormendy 1979), outside of which two broad diffuse arms form a large outer ring. NGC 7217 is similar but even more interesting: although classified as (R)SA(r)ab, NGC 7217 gives the impression of being a series of concentric rings or pseudorings. The principal rings are a very small, high-surface-brightness inner ring and what appears to be an outer ring of the same shape. Between these two rings there is a tight, multiarmed spiral pattern which ends so abruptly that it gives the impression of being a pseudoring or lens. Because the inner rings are so small compared to the extent of the outer structure, both NGC 1068 and 7217 have X values in excess of 1 ($D_0/D_r > 10$).

Two other examples of this behavior are NGC 3166, classified in the RC1 as SAB(rs)O/a, and NGC 3642, classified as SA(r)bc. NGC 3166 appears to have a fat, oval bulge surrounded by a high-surface-brightness pseudoring, the whole region of which is situated in an extensive envelope of relatively uniform surface brightness. The resulting value of $X = 0.96$ for this galaxy is much higher than the typical value for stage $T = 0$, around 0.54 for SAB galaxies. In NGC 3642 there is

© American Astronomical Society • Provided by the NASA Astrophysics Data System

1980ApJS...44..451D

again a closed ring around the center that is small compared to the very extensive outer spiral structure. The value of $X=1.13$ for this galaxy is also much higher than the mean for stage $T=4$ (about 0.81) for SA galaxies.

Finally, a few cases appear either to be misclassifications or possibly the measurements refer to a structure incorrectly described as a ring. Cases where the former may be true are NGC 3182 and 7252. Of these, NGC 7252 is especially peculiar. Although an inner ring structure does appear to be present in this galaxy (as seen on POSS O-plate), outside the ring there is complicated structure, including a long streamer pointing northwest (visible on both E- and O-plates). In the cases of NGC 3182 and 4689, the ring measurement may refer to a spurious ring.

iii) *X and Y as Measures of Bar Strength*

The results of § IV*b*(i) show that our parameters X and Y have a significant dependence on family among the spirals. We need to discuss this point in more detail, and also justify our consideration of the refined family classifications which were used in the least squares solutions.

The family dependence of X and Y was shown to be such that these parameters decrease from SA to SB, with SAB galaxies generally intermediate in value between these extremes. But to study the family dependence more carefully and, in particular, to see if the refinements are significant, it is useful to correct X and Y for their type dependence. This was done using equations (7a) and (7b), where we define $X''=X-0.036T$ and $Y''=Y-0.059T$, which effectively reduces the values of X and Y to $T=0$. The results of these reductions (for the same three cases as were considered in Tables 7, 8, and 9) are collected in Table 10, where values of $\langle X''\rangle$ and $\langle Y''\rangle$ are given as functions of the refined family classification used in the least squares solutions. Table 10 shows that the refinements in the family classification are probably significant; there is a general decrease from SA to SB, and the intermediate families, SAB and SAB, have roughly intermediate values between those of the "main" families (including SAB). Naturally, the statistics of the SAB and SAB families suffer from small numbers since in the classification process there is a strong tendency to assign galaxies more often to the main types (A, AB, B) which leads to a deficiency of transition types. Nevertheless, we believe the data justify our coding of family into a numerical index, and that a linear relationship with family is reasonable, although Table 10 does not necessarily demonstrate a linear relation. Within the mean errors, however, nonlinear representations are not significantly better, and the small relative error of the slope coefficient, $\sigma(a_1)/a_1 \approx 0.015/0.13 = 12\%$, implies a highly significant parameter.

TABLE 10

VALUES OF $\langle X''\rangle$ AND $\langle Y''\rangle$ AS FUNCTIONS OF FAMILY[a]

Family	$\langle X''\rangle$ (m.e.)	N	$\langle Y''\rangle$ (m.e.)	N
	Sample (*a*)			
SA.....	+0.638 ±0.024	66	+0.093 ±0.039	27
SAB	+0.615 ±0.030	41	+0.029 ±0.045	15
SAB	+0.525 ±0.018	85	+0.008 ±0.028	37
SAB	+0.480 ±0.022	41	−0.031 ±0.036	15
SB.....	+0.394 ±0.010	130	−0.150 ±0.020	49
	Sample (*b*)			
SA.....	+0.638 ±0.026	59	+0.090 ±0.044	24
SAB	+0.625 ±0.033	23	+0.044 ±0.052	10
SAB	+0.527 ±0.019	83	+0.013 ±0.028	35
SAB	+0.516 ±0.022	31	+0.018 ±0.037	11
SB.....	+0.393 ±0.010	124	−0.152 ±0.020	46
	Sample (*c*)			
SA.....	+0.682 ±0.039	30	+0.086 ±0.051	16
SAB	+0.657 ±0.041	16	+0.045 ±0.058	9
SAB	+0.547 ±0.024	49	+0.023 ±0.034	27
SAB	+0.529 ±0.023	22	−0.018 ±0.035	9
SB.....	+0.405 ±0.014	73	−0.127 ±0.026	27

[a] Here $X''=X-0.036\,T$ and $Y''=Y-0.059T$ (eqs. [7a] and [7b]).

NOTES—Sample (*a*): All spirals, no rejections. Sample (*b*): Excluding (*rs*) types, no rejections. Sample (*c*): Excluding (*Rs*) types, $D_0 \leq 2.0$, $\log R_{25} > 0.20$, no rejections.

From this analysis we see that X and Y are in some way measures of bar strength and that they indicate that the classification concept of family is in fact a continuous parameter F which can be quantified, at least for galaxies possessing rings. It should be noted that by bar strength we are not necessarily referring to a measure of surface brightness, although this certainly would play a role in the recognition of a bar. Rather, we prefer to think of bar strength as a measure of the character of the bar, i.e., its morphological appearance. For example, a pure barred spiral is generally recognized from the presence of a relatively narrow, straight,

© American Astronomical Society • Provided by the NASA Astrophysics Data System

1980ApJS...44..451D

luminous enhancement which crosses the center; the term bar is obviously applicable in such a case. But among the weakly barred galaxies, denoted SAB in the revised Hubble system, a wider range of forms is possible. These can range from pointed ovals, such as is found in NGC 6744 classified as SAB(r)bc (de Vaucouleurs 1963b) to relatively fat elliptical structures, such as are found in NGC 4303 [SAB(rs)bc] and NGC 4725 [SAB(r)ab], and, further, to relatively small elliptical distortions such as are found in NGC 1232 [SAB(rs)c] and NGC 3310 [SAB(r)bc]. NGC 4303, 4725, and 1232 are illustrated in the *Hubble Atlas* (Sandage 1961); photographs of NGC 3310 are given by Bertola (1965) and by Walker and Chincarini (1967). Beyond the SAB galaxies ($F = -0.5$) we arrive at the pure axisymmetric, or nonbarred (SA) galaxies ($F = -1$). The implication of our result is that the character of the central structure in a spiral galaxy evidently has an important influence on the size of the ring relative to the galaxy. In fact, we will show in Paper II that this "family" effect is present in the *linear* diameters of rings, and that F can be used to quantify this family dependence in the calibration of inner rings as extragalactic distance indicators.

iv) *The Family Dependence of the Scatter in the* (X, Y)–T *Correlations*

It was noted in § IVb(i) that the scatter in the data points of the correlations of X or Y versus T has an apparent dependence on family in the sense that the scatter is smallest for SB galaxies and is largest for SA galaxies. In view of the importance of these parameters for the calibration of rings as distance indicators, it is worth considering the causes of this scatter. In the case of the SAB galaxies, it would be anticipated that a larger dispersion would occur because of the wider range of forms that would be called SAB by galaxy classifiers, as was discussed in § IVb(iii). But the case of the SA galaxies is not so clear. It could be that some of the scatter among the SA galaxies is caused by failure to recognize a weak bar due to insufficient plate material.[5] As was discussed in § IVb(ii) a number of the most discrepant SA galaxies in our sample may possess very weak bars; these galaxies also possess the low values of X consistent with barred spirals. It is possible that in these galaxies the bar was once stronger but has almost completely evolved to an axisymmetric state. Such a speculation has recently been put forth by Kormendy (1979) on the basis of a detailed morphological study of barred galaxies. It could be that some nonbarred galaxies with large rings and small values of X once possessed bars, and that the bar has evolved away leaving behind a ring with a lens filling the region between the central spheroid structure and the ring; such a galaxy might then be classified SA(r).

Another possibility is that the large scatter in the X, Y versus T correlations for SA galaxies is in part due to simple classification errors. It was noted earlier (§ IIc) that spiral arms can mimic ring structures in galaxies especially on plates affected by overexposure or poor resolution. Such false ring structures would make both X and Y too low for a galaxy, and the problem would be most serious for SA galaxies where real inner rings can be completely lost if the center of the galaxy is overexposed; such a recognition problem is not likely to occur for SB spirals, where the rings are of considerably larger relative size.

On the other hand, the large scatter in the X, Y versus T correlations for SA galaxies could also be partly due to a large intrinsic cosmic dispersion in the linear diameters of rings when they form in the absence of bars. Kormendy's speculation cannot explain the pronounced family dependence of X and Y, for if SA(r) galaxies originate through a process of secular evolution from SB(r) galaxies, then both X and Y, as well as the linear diameters of rings, should have no dependence on family, unless the ring by some process changes its diameter during the course of the evolution. It may be that rings can form by a resonance process in the absence of bars, or that more than one mechanism is possible in such cases. Considering the many different mechanisms which have been proposed for forming rings in galaxies (e.g., viscous effects, trapped particle orbits, explosive nuclear phenomena, Lindblad resonance), it may be that no single theory can explain all inner rings.

Finally, the relatively small scatter in the X, Y versus T correlations for the barred spirals could be indicating that rings in barred galaxies are formed by a single mechanism of relatively small cosmic dispersion. Recent theories of galaxy structure have indicated that bars are very conducive to forming rings simply by a redistribution of matter in the disk. Considering the success of particle orbit models such as those of Duus and Freeman (1975) or of the self-gravitating gas flow models of Huntley (1980) in describing barred galaxy structure, it seems that the formation of rings around bars is not too difficult to explain.

v) *A Check on the Classification of the Galaxy*

For obvious reasons, our Galaxy is difficult to classify directly. Early radio studies indicated that the Galaxy is probably a spiral, but the gross details of the morphology were not clear. More recent radio studies have indicated that a weak bar, and possibly even a pseudoring structure, are present near the galactic center. These features led de Vaucouleurs (1964, 1970)

[5]Although M31 is almost a pure (s) variety spiral, and is often taken as typical of the SA(s) family, it is a good example of a weak bar structure barely recognizable on B band photographs (Lindblad 1956), but conspicuous in UV images where it appears as a two-armed SB(s) system (Golay 1979).

© American Astronomical Society • Provided by the NASA Astrophysics Data System

1980ApJS...44..451D

to suggest that our Galaxy is probably an AB(rs)-type spiral, possibly near stage Sb or Sbc. A recent photometric study by de Vaucouleurs and Pence (1978) has quantitatively confirmed this suggestion. In this study the photometric and effective parameters of the Galaxy were estimated by a variety of methods and compared with those of other galaxies of known morphology. The conclusion was that the most probable classification of the Galaxy is SAB(rs)bc, with photometrically derived diameters $D_0 = 23$ kpc and $A_e = 10$ kpc, and with a ring diameter $D_r = 6$ kpc. At the same time it was found that the type and absolute magnitude of the Galaxy, as well the isophotal and effective diameters, are consistent with a luminosity index $\Lambda = (T+L)/10 = 0.71$ (later corrected to 0.66, see *A.J.* **85**, 182).

The values of D_0, A_e, and D_r derived by de Vaucouleurs and W. D. Pence can be used to check the classification of our Galaxy, since, as we have seen earlier in this section, D_0/D_r and A_e/D_r are sensitive to both family and type. Considering once again our dimensionless parameters, we derive for the Galaxy $X_G = 0.58$ and $Y_G = 0.22$. For comparison, we show in Table 11 grids of X and Y values for types $3 \le T \le 5$ over the whole "family sequence" $-1 \le F \le 1$, derived from our least squares solutions (eqs. [7a] and [7b]). Section (a) of Table 11 shows that the value of X for the Galaxy is clearly inconsistent with $F \le 0.0$, i.e., SAB, SAB, and SA are ruled out at all three stages. The classification inferred from the X grid lies on a contour from SABb to SBc, with an approximate intermediate value of SABbc. Section (b) of Table 11 shows that the value of Y for the Galaxy is inconsistent with $F = -1$, and that it lies roughly on a contour going from SABb to SABc, with an intermediate value slightly to the right of SABbc. Clearly, the inferred morphology of our Galaxy based on the X and Y parameters is consistent with the classification SAB(rs)bc determined from the previous studies. In Paper II, we will show that this consistency holds even for the *linear diameter* of the ring, where it will be shown that the Galaxy lies in the domain of the SAB, SB galaxies.

TABLE 11

VALUES OF X AND Y FOR $3 \le T \le 5$

T \ F	-1.0	-0.5	0.0	+0.5	+1.0
	a) X: equation (7a)[a]				
3	0.78	0.71	0.65	0.58	0.52
4	0.81	0.75	0.68	0.62	0.55
5	0.85	0.785	0.72	0.655	0.59
	b) Y: equation (7b)[a]				
3	0.32	0.25	0.19	0.12	0.06
4	0.38	0.31	0.25	0.18	0.12
5	0.435	0.37	0.305	0.24	0.175

[a] Dashed lines show loci of Galaxy ($X_G = 0.58$, $Y_G = 0.22$).

c) Dependence on Corrected Luminosity Class L_c

Corrected luminosity classifications, L_c, calculated according to formulae given by de Vaucouleurs, de Vaucouleurs, and Corwin (1978), are available for 179 of the galaxies in our sample. To complete our analysis of the dimensionless systematics of inner rings, we have studied the dependence of the parameters X, Y and X', Y' on L_c. Since X, Y and X', Y' differ only by a family-dependent term, we illustrate only the dependence of the reduced parameters X', Y' on L_c; these are shown in Figures 21*a* and 21*b*. The graphs show that X' is constant over the range of luminosity classes $0.7 \le L_c \le 8.3$, while Y' is almost constant over the range $0.9 \le L_c \le 7.2$. Thus X' and Y' apparently do not depend on luminosity class. To check these results

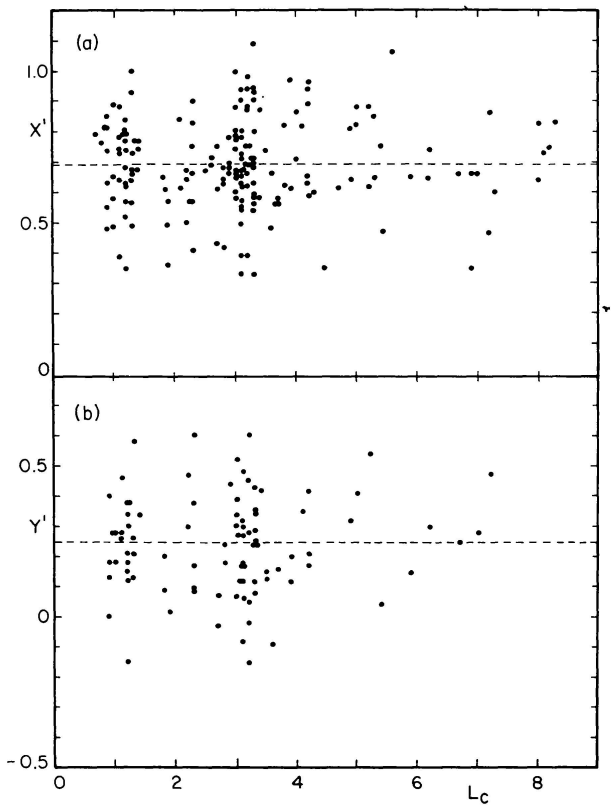

FIG. 21.—X' and Y' versus corrected luminosity class L_c for 179 and 91 spiral galaxies, respectively, having $T \ge 2$. The dashed horizontal lines in each case represent the mean values over the entire range of L_c. There is no significant dependence on L_c.

© American Astronomical Society • Provided by the NASA Astrophysics Data System

1980ApJS...44..451D

TABLE 12

COEFFICIENT a_3 OF EQUATION (10)

Parameters	Coefficient a_3 (m.e.)	N	σ
	Sample (a)		
X	−0.010 ±0.006	171	0.13
Y	−0.004 ±0.012	89	0.15
	Sample (b)		
X	−0.006 ±0.006	147	0.12
Y	−0.003 ±0.012	78	0.15
	Sample (c)		
X	−0.008 ±0.008	98	0.12
Y	−0.013 ±0.014	56	0.14

NOTES—Sample (a): All spirals with $T \geq 2$, after 2σ rejection of NGC 2701, 4051, 4689, 5172, 5248, 5660, 5669, and 7217 from the X solution and NGC 2701 and 5248 from the Y solution. Sample (b): Excluding (rs) types, and after 2σ rejection of NGC 2701, 3642, 4389, 4689, 5172, 5669, and 7217 from the X solution and NGC 2701 and 3486 from the Y solution. Sample (c): Excluding (rs) types, galaxies having $D_o \leq 2'.0$, $\log R_{25} > 0.2$, and after 2σ rejection of NGC 2701, 4689, 5669, and 7217 from the X solution and NGC 2701 and 3486 from the Y solution.

quantitatively, solutions of the form

$$X, Y = a_0 + a_1 F + a_2 T + a_3 L_c, \qquad (10)$$

were calculated for galaxies having $T \geq 2$, and the resulting values for the coefficient a_3 only are collected in Table 12. It is seen that although the coefficient is always negative, it is not significantly different from zero. This result justifies the absence of an L_c term in equations (7a) and (7b).

The lack of significant dependence of X and Y on L_c has two interesting implications. The first is that the linear diameters of inner rings must have the same dependence on L_c as do D_o and A_e. That is, at a given type and family the ring diameter scales exactly with the isophotal or effective diameter at a given luminosity class; there is no residual luminosity class dependence such as there is with type. The second implication is that $\log D_o/A_e$ does not depend significantly on L_c either, at least over the luminosity class range $0.0 \leq L_c \leq 7.0$. This was checked, and the result is illustrated graphically in Figure 22, where mean values of

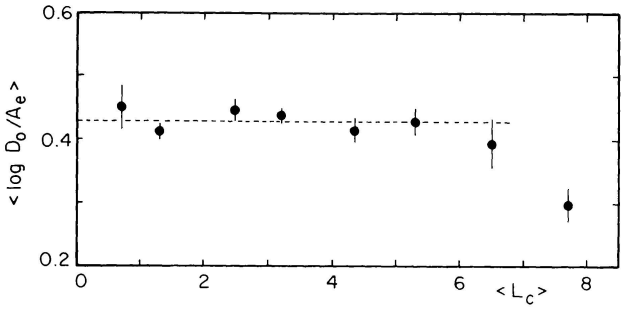

FIG. 22.—Mean logarithmic diameter ratio $\langle \log D_o/A_e \rangle$ vs. mean corrected luminosity class $\langle L_c \rangle$ for 177 RC2 galaxies. The means refer to 8 unit intervals of L_c after rejection of three highly discrepant objects (NGC 1964, 3310, 4736). The dashed line shows the constant mean value of $\log D_o/A_e$ in the interval $0 \leq L_c \leq 7$.

$\log D_o/A_e$ for 180 RC2 galaxies (unrestricted by family or variety) are plotted versus L_c. Figure 22 shows that over most of the range of L_c, $\log D_o/A_e$ is virtually constant; a hint of a dependence is present only at the fainter luminosity classes ($L_c > 6$), but there are not enough points at $L_c > 6$ having A_e values in our ring sample to show an effect of this drop off, for example, on the Y parameter solution. The suggestion from the (X', L_c) plot in Figure 21a is that X', at least, has no dependence on L_c over the full range of luminosity classes found for ringed galaxies.

From the results of this analysis we would conclude that equations (7a) and (7b) imply that the *linear* diameters of inner rings must depend on type, family, and luminosity class. Equation (7a), especially, implies the following form of the relationship:

$$\log D_l(r) = a + bF + cT + dL_c, \qquad (11)$$

for spirals having $T \geq 2$ only. A dependence on L_c is implied because $\log D_o$ depends on L_c (as well as T). In fact, de Vaucouleurs (1979a) has shown that $\partial \log D_o / \partial \Lambda_c = -0.60$, which indicates a slope $\partial \log D_o / \partial L_c = -0.06$. It is interesting to note further that the X solution implies that $\log D_l(r)$ has different slopes with T and L_c; that is, $c \neq d$ so that there is not strictly a Λ_c dependence as there is with the isophotal galaxy diameter. Equation (7a) and the value $\partial \log D_o / \partial \Lambda_c = -0.60$ would seem to imply that $c \approx -0.096$ and $d \approx -0.06$. However, we defer further discussion of these coefficients to Paper II.

Finally, it is important to note that the inferred equation (11) indicates that the ring diameters can be used as distance indicators, albeit only as quaternary indicators. This is because they scale so closely with isophotal and metric diameters of galaxies, both of which have been calibrated as tertiary geometric distance indicators (de Vaucouleurs 1979a, b). This result does not really conflict with Kormendy's (1979) conclusion that inner rings in barred spirals cannot *by them-*

© American Astronomical Society • Provided by the NASA Astrophysics Data System

1980ApJS...44..451D

selves be used as distance indicators because they obey a relation of the form $M_B + 5 \log D_l(r) = \text{constant}$, where M_B is the total blue absolute magnitude of the galaxy. This is merely another expression of the proportionality between galaxy and ring diameters. However, equation (11) shows that *in conjunction* with other information (F, T, L_c), the linear ring diameters can be calculated and used as distance indicators with a precision which will be evaluated in Paper II.

V. SUMMARY AND CONCLUSIONS

We have described in this paper the major morphological properties of inner ring structures in galaxies. New statistical analyses of the relative frequency $f(r)$ of both pure and pseudo inner rings have demonstrated that selection effects due to apparent diameter and especially inclination must be carefully considered. Our statistics of more than 500 RC2 spiral galaxies having large diameters ($D_o > 2'.0$) and reasonably favorable inclinations ($i \leq 50°$) show that pure inner rings (r) are most common among the barred spirals, where $f(r) = 30\%$, and are least common among the nonbarred spirals, where $f(r) = 15.5\%$. We have also suggested that the high relative frequency of pseudo inner rings (rs) among the mixed spiral family (SAB) is a classification artifact due to the central location of this form in the revised Hubble classification volume; classification difficulties also cause serious systematic errors in the apparent frequency of rings among near edge-on lenticulars.

A comparison between the axial ratios of the ring and of the parent galaxy for more than 350 RC2 galaxies has shed some light on the degree of flatness of the rings, but not much on their intrinsic shape in their own plane. Evidently, rings are flat structures in the plane of a galaxy, although we have no information on their intrinsic thickness. However, a comparison of axial ratios for a number of barred spirals with favorable orientation suggests that inner rings in barred spirals may be intrinsically elongated, with the bar as major axis.

A comparison of our data for ring diameter and axis ratio with 43 SB galaxies measured by Kormendy shows good agreement, and indicates that measuring errors will not be a major cause of dispersion in a distance scale based on ring diameters.

Statistical analyses of the dimensionless parameters $X = \log D_o / D_r$ and $Y = \log A_e / D_r$ have revealed strong dependences of these two variables on type and family among the spiral galaxies, and much weaker or less significant dependences on variety and luminosity class. That the ring diameters are largely responsible for the family dependence in these parameters is indicated by the equality of $\partial X/\partial F$ and $\partial Y/\partial F$ in our least squares solutions. In fact, the decrease in X and Y by nearly 0.3 from SA to SB implied by these solutions indicates that rings are a factor of 2 smaller in SA spirals; this result is independent of an extragalactic distance scale. The dependence of X and Y on type indicate that within a given family, the linear diameters of rings are smaller among the later-type galaxies. However, the absolute value of the change in ring diameter with type cannot be determined from these solutions, since both $\log D_o$ and $\log A_e$ are known to depend on type (de Vaucouleurs 1979*a*).

The goal of this paper has been to lay the groundwork for the calibration of inner rings as quaternary extragalactic distance indicators. Their potential for such use, which was first proposed more than 20 years ago (de Vaucouleurs 1956*b*), appears to be considerably strengthened by our analysis. We have shown on the basis of dimensionless systematics that the linear diameters of both pure and pseudo inner rings in spirals later than $T = 2$ depend on type T, family F, and luminosity class L, the strongest dependence being on family. We call attention to the possibility that other statistical properties of galaxies may depend on family. The actual calibration of the ring diameters as extragalactic distance indicators will be performed in Paper II using the recently developed distance scale based on tertiary distance indicators (de Vaucouleurs 1979*a*, *b*), and 21 cm line widths (Bottinelli *et al.* 1980).

We thank Drs. J. Wray and P. Griboval for permission to use their image tube and electronographic plates to prepare Figures 1–3. This work was supported in part by grants from the National Science Foundation the latest being AST 79-16335. One of us (R.B.) also acknowledges the support received from the University of Texas through a David A. Benfield scholarship during the early stages of this work.

APPENDIX

FAMILY INDEPENDENCE OF GALAXY DIAMETERS

We have stated in § IV*b*(i) that the family dependence of the X and Y parameters reflects a dependence of the linear ring diameter D_r on family F, not a variation of D_o or A_e with family (A, AB, B). Although the equality of the slopes $\partial X/\partial F$ and $\partial Y/\partial F$ as well as the lack of family dependence in the $\log D_o/A_e$ parameter (Fig. 20) seem to suggest this, they do not necessarily prove it since D_o and A_e may depend on family in an identical manner which would not be detected in the dimensionless ratios. To check the absolute dependence of these diameters on family, the reduced isophotal and effective (metric) diameters $D_o(1)$ and $A_l(1)$, as defined

© American Astronomical Society • Provided by the NASA Astrophysics Data System

1980ApJS...44..451D

TABLE 13

MEAN REDUCED ISOPHOTAL DIAMETER VERSUS FAMILY FOR 426 SPIRALS[a]

Family	$\langle \log D_o(1) \rangle$	m.e.	σ	N
SA.....	4.144	±0.005	0.063	141
	4.144	±0.004	0.050	135[b]
SAB	4.147	±0.004	0.052	158
	4.146	±0.004	0.045	151[c]
SB.....	4.146	±0.006	0.063	127
	4.145	±0.004	0.047	118[d]

[a]Diameter in parsecs based on μ_0^w distance moduli.
[b]N45, 1084, 1337, 2541, 4414, 6215 2σ rejected.
[c]N247, 1421, 1667, 5236, 5457, 7424, A0102−06 2σ rejected.
[d]N1569, 1744, 3319, 4236, 4449, 5464, 6221, I1727, I5201 2σ rejected.

TABLE 14

MEAN REDUCED EFFECTIVE DIAMETER VERSUS FAMILY FOR 168 SPIRALS[a]

Family	$\langle \log A_I(1) \rangle$	m.e.	σ	N
SA.....	3.748	±0.017	0.124	54
	3.755	±0.016	0.113	53[b]
SAB	3.789	±0.017	0.140	70
	3.802	±0.014	0.114	68[c]
SB.....	3.765	±0.024	0.159	44
	3.778	±0.021	0.136	43[d]

[a]Diameter in parsecs based on μ_0^w distance moduli.
[b]N4736 2σ rejected.
[c]N1964, 3310 2σ rejected.
[d]N1569 2σ rejected.

in Papers V and VI of the distance scale series (de Vaucouleurs 1979*a*, *b*), were calculated for each family using distance moduli μ_0^w derived from tertiary indicators. The reduced diameters are used to remove the dependence of diameters on luminosity index Λ_c. The values of $D_o(1)$ are based on an expanded version of Table 1 in Paper VI (de Vaucouleurs 1979*b*) which includes additional μ_0^w distance moduli for most of the galaxies that did not have a total magnitude or radial velocity in Paper VI; nearly 430 galaxies with μ_0^w were available in the expanded list. The values of $A_I(1)$ are based on the 168 galaxies listed in Table 4 of Paper VI. In both cases, the logarithmic means $\langle \log D_o(1) \rangle$ and $\langle \log A_I(1) \rangle$ before and after 2σ rejection are given in Tables 13 and 14.

It is clear that both the linear isophotal galaxy diameters $D_o(1)$ as well as the metric diameters $A_I(1)$ do not depend significantly on family. In fact, these diameters are remarkably constant irrespective of family. We conclude that the family dependence in the X and Y parameters reflects only a variation in the ring diameters and not in galaxy diameters.

REFERENCES

Benedict, G. F., Van Citters, G. W., McGraw, J. T., and Rybski, P. M. 1977, *Bull. AAS*, **9**, 629.
Bertola, F. 1965, *Contr. Asiago Obs.*, No. 172.
Bosma, A., Ekers, R. D., and Lequeux, J. 1977, *Astr. Ap.*, **57**, 97.
Bosma, A., van der Hulst, J. M., and Sullivan, W. T. 1977, *Astr. Ap.*, **57**, 373.
Bottinelli, L., Gouguenheim, L., Paturel, G. and de Vaucouleurs, G. 1980, *Ap. J. (Letters)*, in press.
Corwin, H. G., Jr., de Vaucouleurs, A., and de Vaucouleurs, G. 1977, *A.J.*, **82**, 557.
_____. 1978, *A.J.*, **83**, 1566.
Curtis, H. D. 1918, *Pub. Lick Obs.*, **13**, Part I, 12.
de Vaucouleurs, G. 1956*a*, *Occasional Notes R.A.S.*, **3**, No. 8, 118.
_____. 1956*b*, *Mem. Com. Obs. Mt. Stromlo*, **3**, No. 13.
_____. 1957*a*, *A.J.*, **62**, 13.
_____. 1957*b*, *L'Exploration des Galaxies voisines*, (Paris: Masson).
_____. 1958, *A.J.*, **63**, 253.
_____. 1959*a*, *A.J.*, **64**, 397.
_____. 1959*b*, *Ann. Obs. Houga*, **2**, No. 2.
_____. 1959*c*, *Handbuch der Physik*, **53**, 275.
_____. 1963*a*, *Ap. J. Suppl.*, **8**, 31.
_____. 1963*b*, *Ap. J.*, **138**, 934.
_____. 1964, in *IAU Symposium No. 20, The Galaxy and the Magellanic Clouds*, ed. F. J. Kerr and A. W. Rodgers (Canberra: Australian Acad. Sci.), p. 195.
de Vaucouleurs, G. 1966, in *Atti Convegno sulla Cosmologia*, (Firenze: Barbiera), p. 37.
_____. 1970, in *IAU Symposium No. 38, The Spiral Structure of our Galaxy*, ed. W. Becker and G. Contopoulos (Dordrecht: Reidel), p. 18.
_____. 1972, in *IAU Symposium No. 44, External Galaxies and Quasi-Stellar Objects*, ed. D. S. Evans (Dordrecht: Reidel), p. 353.
_____. 1975*a*, *Ap. J. Suppl.*, **29**, 193.
_____. 1975*b*, in *Galaxies and the Universe, Stars and Stellar Systems*, Vol. **9**, ed. A. Sandage, M. Sandage, and J. Kristian (Chicago: University of Chicago Press), Addendum, p. 597.
_____. 1977, in *The Evolution of Stars and Galaxies*, ed. B. Tinsley and R. Larson (New Haven: Yale University Observ.), p. 43.
_____. 1979*a*, *Ap. J.*, **227**, 380.
_____. 1979*b*, *Ap. J.*, **227**, 729.
de Vaucouleurs, G. and Buta, R. 1980, *A.J.*, **85**, 637.
de Vaucouleurs, G. and de Vaucouleurs, A. 1964, *Reference Catalogue of Bright Galaxies*, (Austin: University of Texas Press) (RC1).
de Vaucouleurs, G., de Vaucouleurs, A., and Corwin, H. G., Jr. 1976, *Second Reference Catalogue of Bright Galaxies* (Austin: University of Texas Press) (RC2).
_____. 1978, *A.J.*, **83**, 1356.
de Vaucouleurs, G. and Freeman, K. C. 1972, in *Vistas in Astronomy*, Vol. **14**, ed. A. Beer (Oxford: Pergamon Press), p. 259.

© American Astronomical Society • Provided by the NASA Astrophysics Data System

1980ApJS...44..451D

de Vaucouleurs, G., and Pence, W. D. 1978, *A.J.*, **83**, 1163.
de Vaucouleurs, G., and Peters, W. L. 1968, *Nature*, **220**, 868.
Dostal, V., and Metlov, V. 1978, in *IAU Symposium No. 79, The Large Scale Structure of the Universe*, ed. M. S. Longair and J. Einasto (Dordrecht: Reidel), p. 161.
Dressler, A., and Sandage, A. 1978, *Pub. A.S.P.*, **90**, 5.
Duus, A., and Freeman, K. C. 1975, in *La Dynamique des Galaxies Spirales*, ed. L. Weliachew (Paris: CNRS), p. 419.
Freeman, K. C., and de Vaucouleurs, G. 1974, *Ap. J.*, **194**, 569.
Flammarion, C. 1920, *L'Astronomie*, **34**, 534.
Golay, M. 1979, private communication.
Holmberg, E. 1946, *Medd. Lund Astr. Obs.*, Ser. 2, No. 117.
Huntley, J. 1979, 1980, *Ap. J.*, **238**, 524..
Kormendy, J. 1979, *Ap. J.*, **227**, 714.
Lassell, W. 1866, *Mem. R.A.S.*, **36**, 33.
Lindblad, B. 1956, *Stockholm Obs. Ann.*, **19**, No. 2.
Lynds, B. T., Furenlid, I., and Rubin, J. 1973, *Ap. J.*, **182**, 659.
Lynds, R., and Toomre, A. 1976, *Ap. J.*, **209**, 382.
Mebold, U., Goss, W. M., van Woerden, H., Hawarden, T. G., and Siegmann, B. 1979, *Astr. Ap.*, **74**, 100.
Michard, R. 1979*a*, *Astr. Ap.*, **74**, 206.
_____. 1979*b*, *Astr. Ap. Supple.*, **38**, 245 .
Parsons, C. 1926, *The Scientific Papers of William Parsons, Third Earl of Rosse* 1800–1867 (London: The Country Press).
Perrine, C. D. 1922, *M.N.R.A.S.*, **82**, 486.
Randers, G. 1940, *Ap. J.*, **92**, 235.
Sandage, A. R. 1961, *The Hubble Atlas of Galaxies*, Carnegie Institution of Washington Publication No. 618.
_____. 1975, in *Galaxies and the Universe, Stars and Stellar Systems*, Vol. **9**, ed. A. Sandage, M. Sandage, and J. Kristian (Chicago: University of Chicago Press), p. 1.
Sandage, A., and Brucato, R. 1979, *A.J.*, **84**, 472.
Sandage, A. R., and Visvanathan, N. 1978, *Ap. J.*, **225**, 742.
Schommer, R. A., and Sullivan, W. T. 1976, *Ap. Letters*, **17**, 191.
Theys, J. C., and Spiegel, E. A. 1976, *Ap. J.*, **208**, 650.
van den Bergh, S. 1960*a*, *Ap. J.*, **131**, 215.
_____. 1960*b*, *Ap. J.*, **131**, 558.
van der Kruit, P. C. 1976, *Astr. Ap.*, **52**, 85.
Visvanathan, N. and Griersmith, D. 1979, *Ap. J.*, **230**, 1.
Vorontsov-Velyaminov, B. A. 1976, *Pis'ma Astr. Zh.*, **2**, 523.
Walker, M. F., and Chincarini, G. 1967, *Ap. J.*, **147**, 416.
Wray, J. D. and de Vaucouleurs, G. 1980, *A.J.* **85**, 1.

© American Astronomical Society • Provided by the NASA Astrophysics Data System